Journal of Hazardous Materials
Volume 404, Part A, 15 February 2021, 124077

Highly decomposed organic carbon mediates the assembly of soil communities with traits for the biodegradation of chlorinated pollutants

Running title: "Soil organic matter and dieldrin degradation" .

Christian Krohn[a], Jian Jin[a*], Jennifer L. Wood[b,c], Helen L. Hayden[d], Matt Kitching[e], John Ryan[f], Piotr Fabijański[g], Ashley E. Franks[b,c] and Caixian Tang[a]*

[a] Department of Animal, Plant and Soil Sciences, Centre for AgriBioscience, La Trobe University, Melbourne Campus, Bundoora Vic 3086, Australia.
[b] Department of Physiology, Anatomy and Microbiology, La Trobe University, Melbourne Campus, Bundoora Vic 3086, Australia.
[c] Centre for Future Landscapes, La Trobe University, Melbourne Campus, Bundoora Vic 3086, Australia.
[d] Agriculture Victoria, Department of Jobs, Precincts and Regions, Centre for AgriBioScience Bundoora, Vic 3083, Australia
[e] Agriculture Victoria, Department of Jobs, Precincts and Regions, Macleod, Vic 3085, Australia
[f] Agriculture Victoria, Department of Jobs, Precincts and Regions, Wangaratta, Vic 3677, Australia.
[g] Agriculture Victoria, Department of Jobs, Precincts and Regions, Ellinbank, Vic 3821, Australia.

This research did not receive any specific grant from funding agencies in the public, commercial, or not-for-profit sectors and there are no competing interests.

Corresponding authors:
Dr Jian Jin and Prof. Caixian Tang
Department of Animal, Plant and Soil Sciences, Centre for AgriBioScience, La Trobe University,
Bundoora, Vic 3086, Australia
Telephone: +61 3 9032 7416
Fax: +61 3 9032 7605
Emails: j.jin@latrobe.edu.au; c.tang@latrobe.edu.au

Abstract

To improve biodegradation strategies for chlorinated pollutants, the roles of soil organic matter and microbial function need to be clarified. It was hypothesised that microbial degradation of specific organic fractions in soils enhance community metabolic capability to degrade chlorinated pollutants. This field study used historic records of dieldrin concentrations since 1988 and established relationships between dieldrin dissipation and soil carbon fractions together with bacterial and fungal diversity in surface soils of Kurosol and Chromosol. Sparse partial least squares analysis linked dieldrin dissipation to metabolic activities associated with the highly decomposed carbon fraction. Dieldrin dissipation, after three decades of natural attenuation, was associated with increased bacterial species fitness for the decomposition of recalcitrant carbon substrates including synthetic chlorinated pollutants. These metabolic capabilities were linked to the decomposed carbon fraction, an important driver for the microbial community and function. Common bacterial traits among taxonomic groups enriched in samples with high dieldrin dissipation included their slow growth, large genome and complex metabolism which supported the notion that metabolic strategies for dieldrin degradation evolved in an energy-low soil environment. The findings provide new perspectives for bioremediation strategies and suggest that soil management should aim at stimulating metabolism at the decomposed, fine carbon fraction.

Keywords

Humic carbon; Microbiology; Persistent organic pollutants; Bioremediation; Metabolic potential, Soil diversity

1. Introduction

A large variety of chemistries of chlorinated pesticides were marketed globally and used extensively for crop protection with peak production around 1955 [1]. International efforts were made to eliminate the use of the most hazardous persistent organic pollutants [2] but these organic pollutants persist in agricultural soils today and continue to limit land-use options while posing long-term health risks [3,4]. Persistent organic pollutants include highly-chlorinated synthetic pesticides, such as dieldrin, and are resistant to microbial degradation leading to extremely slow biodegradation rates in soils. Biodegradation is the most important process for minimising risks of these type of soil pollutants and fundamental for bioremediation technologies and natural attenuation strategies [5,6]. However, it has been recognised that microbial biodegradation of hydrophobic and chlorinated organics is governed by retention processes and linked to the molecular composition of soil organic matter [7–9]. More knowledge is needed to understand how management of soil organic matter composition is associated with the *in-situ* biodegradation processes of these recalcitrant compounds.

A previous field study showed two agricultural pasture soils (0−10 cm) displayed significantly different abilities to dissipate dieldrin after three decades despite having similar soil characteristics with the exception of location and organic matter content [4]. These soils presented an opportunity to investigate factors for dieldrin dissipation revealing that low soil C/N and high microbial-C-to-total-C ratio [10] were associated with greater dissipation of aged dieldrin after three decades of natural attenuation [4]. This suggests that capabilities for the degradation of dieldrin, one of the most persistent organic pollutants, can be predicted by the presence of persistent soil organic matter and by greater microbial C assimilation efficiencies [11]. From laboratory-scale studies, it has emerged that more refractory C sources such as alkali soil extracts provide substrate for a diverse microbial community with greater metabolic capabilities for the degradation of synthetic organic pollutants [12]. It is further evident that persistent or highly decomposed C fractions impose a stronger influence on the degradation of chlorinated pollutants compared to non-chlorinated pollutants, and that microbial community composition is intimately connected to soil C decomposability [8]. Thus, organic matter composition influences the effectiveness of microbial bioremediation strategies utilising organic matter amendments. Currently, it remains undetermined which factors may increase the effectiveness of microbial bioremediation strategies for chlorinated pollutants in surface soils aged over several decades.

This study aimed to improve understanding how *in-situ* biodegradation of dieldrin was associated with soil organic matter fractions, microbial diversity and functional profiles. We assessed the relationship of three carbon fractions with bacterial and fungal diversities as well as the metabolic profiles estimated from bacterial marker genes using PICRUSt2 [13]. It was hypothesised that microbes in soils which comprised of more decomposed C materials had greater metabolic capabilities to degrade dieldrin.

2. Materials and Methods

2.1. Site, soil description and dieldrin and total carbon measurements

Two agricultural surface soils (0−10 cm) of a Kurosol (n = 21) and a Chromosol (n = 15) [14] which comprised of twelve grazed pastures that were subject to the Australian National Organochlorine Residue Management Plan [15] were sampled in April/May 2017. Each sample was a composite of 8−10 soil cores representing a field replicate. Site location and details, sampling procedure and soil physicochemical characteristics were described previously [4]. The Kurosol and Chromosol consisted of seven and five fenced paddocks, respectively, for which detailed records of dieldrin concentrations since 1988 were obtained. The long-term dieldrin loss (%) per paddock was calculated using the difference of the average dieldrin concentrations from 2015/2017 (D15-17). Climate data for the paddocks in the northeast (Kurosol) and southeast (Chromosol) of Victoria was obtained from the nearest weather stations of the Bureau of Meteorology (http://www.bom.gov.au/climate/data/, accessed 22 May 2020) and are available in Table S1.

Dissipation of dieldrin since 1988 has shown to be significantly greater in the Kurosol compared to the Chromosol (Kurosol 73 ±1.5 %, Chromosol 42 ±3.4 %) [4]. It is important to note that residues of dichlorodiphenyltrichloroethane (p,p'-DDT) and its transformation product dichlorodiphenyldichloroethylene (p,p'-DDE) were also present in both soils but were not part of this study. Only dieldrin was applied to all paddocks until 1988, hence dissipation could be estimated more reliably for dieldrin. From the available data,

it was found that p,p'-DDT dissipation since 1988 was also greater in the Kurosol (Kurosol 71 ±1.98%, Chromosol 43.7 ±5.84 %) [4]. Both soil types consisted of a similar texture (Clay, 12 ±0.4 and 10 ±0.4 %; Silt, 37 ±0.7 and 31 ±0.8 %; Sand, 51 ±0.9 and 59 ±1.1 % for Kurosol and Chromosol, respectively), had the similar pH (4.59 ±0.07 and 4.49 ±0.04 (Kruskal-Wallis p = 0.60), for Kurosol and Chromosol, respectively) and were both in the high-rainfall zone with similar annual maximum temperatures (20.9–21.9 ˚C) [4]. Total organic C significantly differed between the two soils (Kurosol 33.3 ±1.05 mg g^{-1}, Chromosol 61.8 ±1.72 mg g^{-1}), and both the C/N and the microbial-C-to-total-C ratios strongly correlated with dieldrin dissipation (R^2 = 0.89 and 0.93, respectively) [4]. For subsequent analyses, samples were grouped into four categories based on long-term dieldrin loss (%) where the loss was either below or above the median dieldrin loss for each soil type with uneven sample sizes per group.

2.2. Soil organic carbon fractions

Soil organic C fractions were predicted from diffuse reflectance spectra. Soil processing and spectra acquisition followed the method set out in Madhavan et al. (2016). Briefly, air-dried soils were sieved (≤ 2 mm) and finely ground in a ball mill (Retsch MM400, Germany). Diffuse reflectance spectra in the mid and near-infrared (MNIRS) spectra (7800−450 cm^{-1} at 8 cm^{-1} resolution) were acquired for all samples using a PerkinElmer Frontier FT-NIR-MIR Spectrometer (PerkinElmer Inc., Waltham, MA, USA) equipped with a KBr beam-splitter, a DTGS detector and AutoDiff automated diffuse reflectance accessory (Pike Technologies, Madison, WI, USA).

Spectra were pre-processed as described in Madhavan et al. (2017) and concentrations of total organic C (total-C), resistant organic C (resistant-C), humic organic C (humic-C) and particulate organic C (particulate-C) were predicted from MNIRS spectra of the Australian Soil Carbon Research Project (ScaRP) [18] using partial least squares (PLS) regression. From these spectra and methodology, resistant-C was defined as the proportion of char and lignin C (enriched in poly-aryl C) in both fine and coarse fractions, and considered to be biologically resistant. Particulate organic C was defined as the remaining coarse fraction (> 50 µm) and was considered to be relatively rich in carbohydrates (enriched in O-alkyl C) and the most biologically active and decomposable. Humic organic C was defined as the remaining fine fraction (< 50 µm) and considered to be low in carbohydrates and more decomposed (enriched with alkyl C) compared to particulate-C [18].

Estimated total-C concentrations from the PLS predictions were correlated with total-C measurements of the same samples using a dry combustion analyzer (Perkin Elmer 2400 Series II, R^2 = 0.98). Hydrogen (H) concentrations were also derived and the hydrogen-to-total-C ratio calculated as approximation for aliphatic C content in downstream analyses. Raw data are shown in Table S2. For all downstream analyses, resistant-C, humic-C and particulate-C were either transformed into percentages of total-C or into centered log ratios.

2.3. Diversity measurements

DNA samples were obtained from the extraction of 0.25 g fresh soil using Powersoil DNA isolation kit (MoBio, Calsbad, USA) and stored at -20 ˚C. Marker genes were sequenced with 15% phiX control on the Illumina MiSeq platform (2 × 300) to determine bacterial and fungal diversity. For bacteria the V4 hypervariable region of the 16S-rRNA gene was targeted with primers 515F (GTGYCAGCMGCCGCGGTAA) / 806R (GGACTACNVGGGTWTCTAAT) [19]. For fungi, the Internal Transcribed Spacer (ITS) region 2 [20] was amplified with primers FITS7 (GTGARTCATCGAATCTTTG)/ITS4 (TCCTCCGCTTATTGATATGC) [21].

The default settings of Qiime2 (v2020.2, https://qiime2.org) were used to assess the quality of paired end reads, trim primers, denoise and dereplicate sequences and filter chimeras (dada2) [22]. Sequences with number of expected errors >2 were discarded and 66% (bacteria) and 52% (fungi) of sequences were retained after filtering. A total of 19,918 and 4,712 unique amplicon sequence variants (ASVs) (bacteria and fungi, respectively) were identified. Qiime2 was then used to train primer-specific classifiers using Greengenes reference sequences (gg13.8 at 99% similarity) for bacteria (https://greengenes.secondgenome.com/) and UNITE reference sequences (v8 dynamic) for fungi (https://unite.ut.ee/) and the classifiers were then used to assign taxonomic classifications to ASVs with 'qiime feature-classifier classify-sklearn'.

For bacterial ASVs, a phylogenetic tree was created using the default options of the Qiime2 plugin q2-fragment-insertion that utilized SATé-enabled phylogenetic placements (SEPP) with the Greengenes 13.8

SEPP reference tree. The tree was subsequently used to calculate the faith phylogenetic diversity index and unifrac metric and for phylogenetic analysis of associations to dieldrin loss as outlined below.

Prior to subsequent community analyses three outliers were removed which belonged to a paddock that was not representative of the remaining paddocks in the Kurosol (final n = 33). To assess differences in diversity between samples with high and low dieldrin losses, alpha diversity indices were produced with phyloseq [23] on rarefied abundances (depth to minimum sample size; 32,417 reads) of bacteria, their predicted enzyme metagenome and fungi. The phyloseq package was used to make compositional comparisons of bacterial, enzyme and fungal abundances in principle component analysis (PCA) and redundancy analysis (RDA) after converting abundance tables into Aitchison distances [24]. ASVs were filtered to those ASVs and enzymes present in at least 25% of samples. This included 1465 and 1705 bacterial ASVs, and 398 and 403 fungal ASVs in the Kurosol and Chromosol, respectively, and further included 2093 enzymes in both soils. To assess the influence of C fractions on bacterial and fungal community composition, resistant-C, humic-C and particulate-C were used as constraining variables in RDA and significance of RDA constraints assessed using 999 permutation of a pseudoF statistic in the function `permutest` of the vegan package [25]. The functions 'betadisper' (vegan package) and 'leveneTest' (car package) were used to test for significantly different compositional dispersion between soils and variation of phylogenetic diversity between samples [26].

2.4. Enzyme metagenome and MetaCyc pathway associations to carbon fractions and dieldrin concentrations

The PICRUSt2 (Phylogenetic Investigation of Communities by Reconstruction of Unobserved States 2) software [13] was used to predict the enzyme metagenome and metabolic pathways (MetaCyc, Karp, 2002) based on the bacterial ASVs. Briefly, the PICRUSt2 pipeline placed ASVs into an open-source reference tree based on prokaryotic genomes from the Integrated Microbial Genomes database [28], inferred gene abundances per ASV and then predicted sample pathway abundances using MinPath. The full pipeline (https://github.com/picrust/picrust2/wiki/Full-pipeline-script) was run with default settings, except that the maximum Nearest Sequence Taxon Index (NSTI) was set to 0.65 in favor of greater accuracy of predictions. Prior to running the PICRUSt2 pipeline, the ASV table was filtered to those ASVs that were present in at least two samples and with a minimum frequency of 10 reads. The final table output comprised of 432 pathway abundances that represented the metabolic potentials of bacteria in each sample.

Sparse partial least squares analysis (sPLS), including sPLS discriminant analysis (sPLS-DA) of the mixOmics package [29] were chosen to explore associations between metabolic pathway potentials and soil variables of resistant-C, humic-C, particulate-C, C/N and dieldrin loss (%). The sPLS is a dimension reduction technique that integrates two high-dimensional data sets acquired from the same samples (here predicted pathway potentials and soil variables) to highlight general patterns of associations. These methods perform well when the number of samples (*n*) is smaller than the measured variables (*p*) and when variables exhibit multicollinearity. For detailed description of approach, see the supplementary section.

2.5. Analysis of phylogenetic associations to dieldrin losses

To test whether the presence of some bacterial clades was more likely associated with dieldrin loss, the package Phylofactor [30] was used to perform generalized phylofactorization with the mixed algorithm and a binomial distribution as described in the package tutorial (https://github.com/reptalex/phylofactor). Phylofactorization was chosen as it has the ability to detect similar shifts in microbial clades among different data (or soils) when mapped to the same phylogeny, even with minimal ASV overlap [31]. The analysis was done across both soils (n = 33) and then separately on each soil type (Kurosol, n=18; Chromosol, n=15). Any unidentified phyla and phyla with low prevalence (mean prevalence of 1 or < 100 reads) were removed. Remaining ASVs filtered to a minimum of 25 reads per ASV and converted to presence/absence, which was modelled as the response variable with dieldrin losses (%) as numeric predictors. Phylofactor partitioned the phylogeny along edges with different log-odds of presence using generalized linear models (default mixed algorithm) with binomial distributions. The identified clades were then mapped onto the phylogenetic tree using ggtree.

2.6. Network analysis of bacterial and fungal co-correlation

To investigate differences in community interactions of unique bacteria and fungi in the Kurosol and the Chromosol, co-correlation networks were created using sparse inverse covariance estimation for ecological

association inference (Spiec-easi) [32] with glasso estimations. After filtering of ASVs to a minimum sample-presence of 25%, bacterial and fungal abundances were co-correlated using a stability approach to regularization selection (StARS) [33] with a threshold of 0.05 and 25 repetitions (other settings: nlambda = 30, lambda minimum ratio = 0.02). Network edges were processed in gephi [34] and nodes of taxa that were unique in samples with above median dieldrin losses were visualised. Furthermore, the average path lengths were calculated and keystone taxa highlighted. Modularity was calculated [35] and strongly interacting bacteria and fungi (modules) identified. Module zero and four coincided with the presence of unique ASVs in samples with above or below median dieldrin loss (%). To investigate ecological preferences of these two groups of taxa, the standardised relative abundance (Z-score) of each module was computed and correlated to organic matter fractions (Spearman).

3. Results

3.1. Carbon decomposition continuum

The two soils, Kurosol and Chromosol, differed in dieldrin dissipation, organic C composition and displayed different metabolic profiles. Samples with higher proportions of highly decomposed or lower quality C materials displayed greater capabilities for degradation of recalcitrant C materials including chlorinated hydrocarbons (Figs 1 and 2). The Kurosol contained significantly less total-C compared to the Chromosol (61.8 ±1.7 g kg^{-1} and 33.7 ±1.0 g kg^{-1}, respectively) but consisted of less charcoal and lignin-like materials (poly-aryl C) as indicated by the smaller resistant-C fraction (28 ±0.3 % and 24 ±0.6 %) (Fig. 1). The Kurosol had significantly greater hydrogen-to-total-C ratios but lower C/N than the Chromosol, indicating that overall the organic matter was enriched in aliphatic C sources and therefore more decomposed (Figs 1 and S1). This aliphatic C stemmed mostly from the humic-C fraction which constituted the biggest C fraction (45 ±0.5 % and 51 ±1.0 % for Chromosol and Kurosol, respectively). The Kurosol also consisted of more fresh, decomposable material than the Chromosol, indicated by the larger particulate-C fraction (4.8 ±0.4 % and 9.5 ±0.6 % for Chromosol and Kurosol, respectively). Altogether, the organic matter in the Kurosol exhibited a higher metabolic potency for the degradation of chlorinated and aromatic carbon sources compared to the Chromosol, which coincided with increased dieldrin dissipation (Fig. 2).

3.2. Associations of MetaCyc pathway potentials with dieldrin dissipation

Abundances of 260 metabolic pathway potentials, which contributed to variations in the first three latent components in sPLS-DA, were predictive of dieldrin dissipation. Of those metabolic potentials, 10 degradation pathways (four carbohydrate, one alcohol, one carboxylate and two polyamine degradation pathways) and a vitamin biosynthesis pathway contributed most to component loadings (Fig. 3). Correlations between metabolic pathways and C fractions from loadings of the first two components from sPLS further showed that the potentials for fucose, rhamnose, lactose, galactose and glycol degradation were most strongly associated with high dieldrin dissipation (Table 1, Fig. S2). In contrast, oxidative glucose degradation was associated with low dieldrin dissipation since 1988 (Fig. 3).

3.3. Compositional associations to dieldrin loss and soil C fractions

The microbial community composition differed between the Kurosol and Chromosol (Fig. S3) and greater dieldrin losses coincided with significantly higher bacterial and fungal richness, as well as enzyme-encoding genes (Fig. S4) and greater microbial diversity per unit of dieldrin (Fig. S5). While the phylogenetic composition of bacteria was similar in the Kurosol and in the Chromosol (Fig. S6–S8), only in the Kurosol were soil C fractions associated with the composition of bacteria, enzymes and fungi (Fig. 4). Permutation tests for the joint effect of resistant-C, humic-C and particulate-C were significant for the Kurosol ($p < 0.001$) but not for the Chromosol ($p > 0.05$). The Kurosol community also contained a higher number of unique ASVs with greater phylogenetic dispersion, suggesting a greater phylogenetic versatility, which coincided with increased dieldrin losses (Figs S6 and S8).

Of the three soil C fractions, humic-C was the biggest driver of community function in the Kurosol. Individual permutation tests for humic-C ($p < 0.01$), resistant-C ($p = 0.07–0.18$) and particulate-C ($p = 0.19–0.45$) in the model indicated that humic-C was most important for bacterial, fungal and the metabolic compositions while

particulate-C was least important (Table 2). The highest dieldrin dissipation (%) occurred in Kurosol samples where the microbial community and metabolic composition was associated with humic-C (Fig. 4). An increase in humic-C was further associated with dieldrin loss and the metabolic potential for the degradation of lactose and galactose (Fig. S2).

3.4. Associations of humic C with a group of bacteria and fungi and dieldrin dissipation

The combined abundance of a co-correlated group of bacteria and fungi in the Kurosol, was associated with humic-C concentrations (R^2 = 0.57***, Figs 5 and S9, Module zero). This cluster was also associated with dieldrin dissipation as it contained a group of bacteria and fungi which were only found in samples with above median dieldrin loss (Fig. 5). Bacterial interactions were generally dominant while fungal interactions increased in another cluster (Module four) which was associated with below median dieldrin loss (Fig. 5; Table S3), indicating that fungal interactions were less influential on high dieldrin degradation.

A number of phylogenetic clades had a significantly higher presence in samples with high dieldrin loss as determined by generalised linear models with presence/absence as response variable (Table S4). These clades included Acidobacteria, Actinobacteria, Bacteroidetes, Chloroflexi, Planctomycetes and *Geobacter sp.* (Table 3, Fig. S7). Most of these were strongly representative of the humic-C-associated cluster (Module zero) of bacteria and fungi (Fig. 5). For example, Actinobacteria in the order Solirubrobacterales were 12 times more frequent, while Planctomycetes in the order Gemmatales were 6 times more frequent in Module zero compared to Module four. Furthermore, Chloroflexi in the order of WCHB1-50 and Bacteroidetes in the order Bacteroidales were unique in Module zero. Of the fungal taxa, one group belonging to the order Hypocreales was the strongest representative for Module zero as it was 13 time more frequent there. The genera *Fusarium*, *Thelonectria*, *Trichoderma*, *Myxocephala* and *Monocillium* dominated in this group.

4. Discussion

4.1. Dieldrin dissipation was linked to a resource-limited soil environment

Two pasture surface soils were investigated, Kurosol and Chromosol, with differing potentials of dieldrin dissipation over the past three decades. An important finding was that metabolic capabilities of microorganisms for degradation of chlorinated pollutants were linked to adaptations to a resource-limited soil environment and driven by highly decomposed C materials. Samples which exhibited high dieldrin dissipation were enriched in aliphatic or lipid-rich C materials as indicated by the C/N and H-to-total-C ratios and humic-C proportions (Fig. 1) [36–38]. We refer to humic-C as the pool of lipid-rich materials (< 50 μm) which were decomposed to small molecules and were energy-poor or physically-protected from microbial degradation [39]. Also known as persistent or mineral-associated organic matter, it is usually the largest fraction of soil organic matter and composed of a complex mixture of microbially-derived detritus [40,41]. Laboratory-scale studies, using synthetic alkali extracts to emulate this C fraction, showed that they provided substrate for a microbial diversity with greater metabolic capabilities for xenobiotic degradation [12]. This is consistent with this field study which showed that highly decomposed soil C (humic-C) coincided with increased potentials for degradation of chlorinated xenobiotics and aromatic compounds (Fig. 2). It was concluded that dieldrin degradation processes were greater in a resource-limited soil environment containing low quality, energy-poor or more decomposed C materials.

This was further associated with increased C assimilation efficiencies, expressed as an increase in the microbial-C-to-total-C ratios [11], as our previous study showed strong correlations of total dieldrin dissipation to high microbial-C-to-total-C ratios (R^2 = 0.93) [4]. These increases in C-use efficiency were likely the result of more efficient maintenance processes of a microbial community that evolved in an energy-low soil environment. According to the model by Xu et al. [11], the efficiency with which microorganisms assimilate C into their biomass is determined by two factors: C assimilation efficiency and maintenance energy requirements over time. Carbon assimilation efficiencies increase with high C quality combined with low maintenance energy requirements. As the soil C quality was lower in samples with increased dieldrin losses, it was concluded that dieldrin degradation was associated with microbial strategies that increase maintenance efficiencies.

More efficient microbial activity can evolve from resource-limitations or seasonal stresses such as high temperatures and drought [11,42,43]. Seasonal stresses in the Kurosol can also explain the lower C stocks (Fig. 1) as the maximum soil C content in a given location is mainly determined by maximum and minimum rainfall and temperature [44–46]. This was consistent with local climate data. In the last three decades, the King Valley region, where the Kurosol samples were taken, had greater extremes and variability in temperatures, rainfall and solar exposure (Table S1). Additionally, decadal floods occurred in seasons with heavy rainfalls. Such environmental stress has shown to increase phylogenetic dispersion of microbial communities [31], which agreed with our data showing an increase of phylogenetic variability with increased dieldrin dissipation (Fig. S8). This supported the suggestion that a stressed or resource-limited soil environment impacted on microbial degradation of dieldrin.

A resource-limited soil environment selects for microbial traits that maximise growth yield, a concept known as rate-yield tradeoff [47]. In the present study, it was observed that the potential for the Entner-Doudoroff pathway was predictive for high dieldrin dissipation (Fig. 3). The Entner-Doudoroff glycolytic pathway is more common than originally thought [48] and it was found that it yielded less energy but required several-fold less enzymatic protein compared to the better known Embden–Meyerhof–Parnas pathway [49], potentially freeing up resources to invest in more complex degradation processes. It was therefore speculated that the limited access to energy and C materials selected for microbial traits which aided in accessing energy-low materials, for example through the production of exoenzyme or extracellular glycolipids and that this increased co-metabolism of dieldrin.

4.2. The highly decomposed carbon C fraction was driving dieldrin dissipation

The persistent and highly decomposed C fraction played a significant role in the dissipation of dieldrin. Among the three C fractions, humic-C was the most significant driver for the microbial community and functional composition in the Kurosol (Fig. 4, Table 2). There were unique associations between bacteria and fungi which demonstrated a preference for this C pool as the combined abundance (Z-score) of a group of co-correlated bacteria and fungi (Gephi modularity, Module zero) increased with humic-C concentrations (R^2 = 0.57***, Figs 5 and S9). By contrast, in the Chromosol there was no effect of the C composition on the microbial community, suggesting that C quality was less important for community dynamics in this soil, which coincided with lower dieldrin dissipation (Figs 4 and 5). Moreover, functional potentials of bacteria in the Kurosol were associated to dieldrin loss and simultaneously associated to humic-C (Table 1, Fig. S2) which further showed that decomposed C materials support soil functions that coincided with dieldrin degradation. Finally, the Kurosol, with greater dieldrin dissipation, contained less organic matter as well as lower proportions of charcoal or lignin materials (resistant-C), suggesting that irreversible sequestration of dieldrin was less pronounced compared to the Chromosol (Fig. 1) [50]. As a result, interactions between humic-C and dieldrin molecules were likely more prevalent in the Kurosol.

Potentials of several metabolic pathways of the bacterial community gave further insights into microbial traits that were associated with highly decomposed C materials and dieldrin dissipation. The sPLS analysis showed that strongest predictors for high dieldrin losses included the metabolic potentials for degradation of microbial sugars such as fucose, rhamnose, lactose and galactose (Fig. 3, Table 1). The concentration of microbial sugars in soils such as those from extracellular rhamnolipids or lipopolysaccharides in the cell membrane is typically five times lower than glucose [51–53]. Microbial sugars have been shown to be enriched in the fine C fraction and protected against microbial degradation, potentially through organo-mineral associations [54,55]. This indicates that the higher microbial maintenance efficiencies in samples with high dieldrin dissipation were associated with metabolic adaptations to utilise microbially-derived C which itself was associated with protected and highly decomposed materials. Microbial biomass itself becomes an important reservoir and buffer of nutrients during stress or resource-limited periods [56], hence the findings supports the idea that these conditions promote degradation of recalcitrant carbon materials including dieldrin. Taken together, dieldrin dissipation was associated with decomposed C materials which mediated community assembly with traits that aided degradation of chlorinated organics.

These data imply that the provision of labile and decomposable C may inhibit biodegradation of chlorinated organics. This was also evident in a long-term field experiment studying the degradation of a chlorinated model compound (2,4-dichlorophenol (DCP)) [8]. Degradation of DCP was associated with the clay fraction (< 2 µm) which comprised a distinct microbial community [57], and it was found that farmyard manure reduced

degradation of DCP as it reduced mass transfer of DCP to relevant microbial cells [8]. Thus, in agreement with our findings, which showed that dieldrin dissipation was associated with the finer C fraction, soil management should aim at stimulating metabolism of the decomposed fine C fraction. These findings offer new perspectives for natural attenuation strategies especially for agricultural surface soils which are contamination with organochlorines for several decades. We speculate that disruption of the soil structure by frequent tillage is needed to stimulate biodegradation of dieldrin by indigenous microorganisms. The rational is that frequent tillage would give microorganisms access to non-labile C, including dieldrin and promote growth of relevant degraders. On the other hand, no-till practices and perennial pastures may delay dieldrin dissipation as labile C sources are constantly provided by rhizodeposites. These recommendations sit in contrast to common soil-health practices which aim at increasing soil organic matter content. Controlled experiments are needed to verify if disturbance of soil structure and microbial communities promote the assembly of microorganisms with desired traits for degradation of chlorinated contaminants under these circumstances.

4.3. Microbial traits in samples with high dieldrin dissipation

Some taxonomic groups were more prevalent in samples with high dieldrin dissipation (Table 3, Fig. S7). An assessment of their traits gave further insights into the potential role of highly decomposed C for the degradation of chlorinated pollutants in surface soils. To measure which phylogenetic groups related to dieldrin dissipation, probabilities of the presence of aggregated ASVs were modelled along the gradient of total dieldrin dissipation (Table S4) [58]. It was found that taxonomic groups which were significantly associated with dieldrin dissipation (Phylofactor, $p < 0.001$) were also prevalent in the group of bacteria and fungi that were driven by humic-C concentrations (Fig. 5). They included aerobic and anaerobic bacteria in the order Acidobacteriales, Solirubrobacterales, Sphingobacteriales, Bacteroidales, Gemmatales and a group of Chloroflexi and *Geobacter sp*. A similar bacterial assemblage was observed in microcosms supplemented with synthetic humic acids and harbored stronger and more diverse capabilities for degradation of organic pollutants [19]. However, fungi were less abundant in the humic-C associated group in the Kurosol (Fig. 5). Instead, fungi were more abundant in another group which was associated with below median dieldrin loss, indicating that fungi were less important for biodegradation of dieldrin (Table S3).

Common traits among these bacteria included their slow growth, large genome, complex metabolism, motility, radiation tolerance and desiccation resistance and these traits may have contributed to increased co-metabolism of dieldrin. Their complex metabolism enabled them to utilise a range of different C sources, including sugars such as fucose, rhamnose, lactose and galactose. For example, the metabolism of a clade in the order of Acidobacteriales, which comprised mostly of the genus *Candidatus Koribacter* (Table 3, Fig. S7), is adapted for nutrient-poor environments and able to utilise complex C substrates at low concentrations [59]. Moreover, the Kurosol contained significantly higher frequencies of bacteria in the order Actinomycetales. Some genera in this order, such as *Pseudonocardia spp*. and *Rhodococcus spp.,* have shown to co-metabolise dieldrin and dichlorodiphenyltrichloroethane (DDT) [60,61]. Furthermore, a group of bacteria in the order Sphingobacteriales was more prevalent in the Kurosol, along with other Bacteroidetes. Some strains of *Sphingobacterium thalpophilum* are known for co-metabolic degradation of pentachlorophenol when grown on glucose [62] while other *Sphingobacterium sp.* were able to utilise DDT as a sole C source [63].

Further groups of strictly anaerobic Chloroflexi, known for their ability to dechlorinate hydrocarbons were unique in the Kurosol and most prevalent in samples with high dieldrin dissipation (Table 3, Fig. S7). They belonged to the class Anaerolineae which comprise filamentous thermophiles with diverse metabolic strategies, including reductive dechlorination of chlorinated hydrocarbons [64]. Lastly, clades of anaerobic Proteobacteria and Firmicutes, which are known to couple their growth to the reduction of humic substances, were significantly more prevalent in samples with high dieldrin dissipation (Table 3, Fig. S7). Both the group of Proteobacteria in the order Desulfuromonadales which comprised exclusively of *Geobacter spp*. and a group of bacteria in the order Clostridiales have shown to degrade chlorinated hydrocarbons in enrichment-culture and microcosms [65,66]. Humic substances acted as catalytic 'electron shuttles' which was coupled to Fe(III) reduction to enhance degradation of these pollutants [67]. Dieldrin dissipation was therefore associated with a microbial community with metabolic capabilities for degradation of complex C substrates including synthetic chlorinated pollutants.

4.4. Conclusions

The results from this field study add to our understanding of potential ecological drivers which affect natural attenuation or bioremediation strategies [5,68]. Two pasture soils, Kurosol and Chromosol, displayed differing potentials of dieldrin dissipation over three decades (72 % and 43 % median dieldrin loss, respectively). The study suggested that dieldrin dissipation was associated with microbial traits that evolved in an energy-low soil environment in which highly decomposed and persistent carbon materials (< 50 µm) mediated microbial community assembly and function. This implies that the provision of labile C could slow down biodegradation of chlorinated organics and that soil management should aim at stimulating metabolism at the decomposed, fine carbon fraction. Field studies at scale are required to validate our findings and to evaluate the impacts of different soil management practices on biodegradation of chlorinated pollutants.

Acknowledgements

Historical data of dieldrin and DDT concentrations were kindly provided by The National Organochlorine Residue Management Program (NORM). We thank Sarah Knowler, Josh Vido, Gene Drendel, Dr. Steven Batinovic and Dr. Steve Petrovski (La Trobe University, Melbourne, Victoria) and Bruce Shelley (Agriculture Victoria, Department of Jobs, Precincts and Regions) for technical advices.

Conflict of Interest

This research did not receive any specific grant from funding agencies in the public, commercial, or not-for-profit sectors. CK received an Australian Government Research Training Program Scholarship.

References

[1] M. Scheringer, Persistence and Spatial Range of Environmental Chemicals: New Ethical and Scientific Concepts for Risk Assessment, Wiley-VCH, Weinheim, Germany, 2002. https://doi.org/10.1002/3527607463.

[2] United Nations Environment Programme (UNEP), Stockholm convention on persistent organic pollutions (POPs), Châtelaine GE, Switzerland, Available at http://chm.pops.int, 2017. http://chm.pops.int (accessed August 20, 2019).

[3] Z. Li, A. Jennings, Worldwide regulations of standard values of pesticides for human health risk control: A review, Int. J. Environ. Res. Public Health. 14 (2017) 826. https://doi.org/10.3390/ijerph14070826.

[4] C. Krohn, J. Jin, J. Ryan, P. Fabijański, A.E. Franks, C. Tang, Composition of soil organic matter drives total loss of dieldrin and dichlorodiphenyltrichloroethane in high-value pastures over thirty years, Sci. Total Environ. 691 (2019) 135–145. https://doi.org/10.1016/j.scitotenv.2019.06.497.

[5] C.N. Mulligan, R.N. Yong, Natural attenuation of contaminated soils, Environ. Int. 30 (2004) 587–601. https://doi.org/10.1016/j.envint.2003.11.001.

[6] R. Boopathy, Factors limiting bioremediation technologies, Bioresour. Technol. 74 (2000) 63–74. https://doi.org/10.1016/S0960-8524(99)00144-3.

[7] Y. Yang, N. Zhang, M. Xue, S.T. Lu, S. Tao, Effects of soil organic matter on the development of the microbial polycyclic aromatic hydrocarbons (PAHs) degradation potentials, Environ. Pollut. 159 (2011) 591–595.

[8] D. Neumann, A. Heuer, M. Hemkemeyer, R. Martens, C.C. Tebbe, Importance of soil organic matter for the diversity of microorganisms involved in the degradation of organic pollutants, ISME J. 8 (2014) 1289–1300.

[9] N. Zhang, Y. Yang, S. Tao, Y. Liu, K.-L. Shi, Sequestration of organochlorine pesticides in soils of

distinct organic carbon content, Environ. Pollut. 159 (2011) 700–705. https://doi.org/10.1016/j.envpol.2010.12.011.

[10] T.H. Anderson, K.H. Domsch, Ratios of microbial biomass carbon to total organic carbon in arable soils, Soil Biol. Biochem. 21 (1989) 471–479.

[11] X. Xu, J.P. Schimel, P.E. Thornton, X. Song, F. Yuan, S. Goswami, Substrate and environmental controls on microbial assimilation of soil organic carbon: A framework for Earth system models, Ecol. Lett. 17 (2014) 547–555. https://doi.org/10.1111/ele.12254.

[12] D. Li, M. Alidina, J.E. Drewes, Role of primary substrate composition on microbial community structure and function and trace organic chemical attenuation in managed aquifer recharge systems, Appl. Microbiol. Biotechnol. 12 (2014) 5747–5756. https://doi.org/10.1007/s00253-014-5677-8.

[13] G.M. Douglas, V.J. Maffei, J. Zaneveld, S.N. Yurgel, J.R. Brown, C.M. Taylor, C. Huttenhower, M.G.I. Langille, PICRUSt2: An improved and extensible approach for metagenome inference, BioRxiv. 175 (2019) 67–75.

[14] R.F. Isbell, The Australian Soil Classification, CSIRO Publishing, Victoria, Australia, 1996.

[15] Department of Natural Resources and Environment (DNRE), History and purpose of the NORM program, manual of procedures, DNRE (1996 - 2002), Victoria, Australia, 1996.

[16] D.B. Madhavan, M. Kitching, D.S. Mendham, C.J. Weston, T.G. Baker, Mid-infrared spectroscopy for rapid assessment of soil properties after land use change from pastures to Eucalyptus globulus plantations, J. Environ. Manage. 175 (2016) 67–75. https://doi.org/10.1016/j.jenvman.2016.03.032.

[17] D.B. Madhavan, J.A. Baldock, Z.J. Read, S.C. Murphy, S.C. Cunningham, M.P. Perring, T. Herrmann, T. Lewis, T.R. Cavagnaro, J.R. England, K.I. Paul, C.J. Weston, T.G. Baker, Rapid prediction of particulate, humus and resistant fractions of soil organic carbon in reforested lands using infrared spectroscopy, J. Environ. Manage. 193 (2017) 290–299. https://doi.org/10.1016/j.jenvman.2017.02.013.

[18] J.A. Baldock, B. Hawke, J. Sanderman, L.M. MacDonald, Predicting contents of carbon and its component fractions in Australian soils from diffuse reflectance mid-infrared spectra, Soil Res. 51 (2013) 577–595. https://doi.org/10.1071/SR13077.

[19] A. Apprill, S. McNally, R. Parsons, L. Weber, Minor revision to V4 region SSU rRNA 806R gene primer greatly increases detection of SAR11 bacterioplankton, Aquat. Microb. Ecol. 75 (2015) 129–137.

[20] R. Blaalid, S. Kumar, R.H. Nilsson, K. Abarenkov, P.M. Kirk, H. Kauserud, ITS1 versus ITS2 as DNA metabarcodes for fungi, Mol. Ecol. Resour. 13 (2013) 218–224. https://doi.org/10.1111/1755-0998.12065.

[21] I. Katarina, B.I. T.M., C. Karelyn, F. Hanna, K. Ariana, S. Jessica, S. Ylva, S. Jan, B. Mikael, C.K. E., L.B. D., New primers to amplify the fungal ITS2 region – evaluation by 454-sequencing of artificial and natural communities, FEMS Microbiol. Ecol. 82 (2012) 666–677. https://doi.org/10.1111/j.1574-6941.2012.01437.x.

[22] B.J. Callahan, P.J. McMurdie, M.J. Rosen, A.W. Han, A.J.A. Johnson, S.P. Holmes, DADA2: high-resolution sample inference from Illumina amplicon data, Nat. Methods. 13 (2016) 581.

[23] P.J. McMurdie, S. Holmes, Phyloseq: A bioconductor package for handling and analysis of high-throughput phylogenetic sequence data, Biocomputing. (2012) 235–246. https://doi.org/10.1142/9789814366496_0023.

[24] J. Aitchison, The Statistical Analysis of Compositional Data, J. R. Stat. Soc. Ser. B. 44 (1982) 139–160. https://doi.org/10.1111/j.2517-6161.1982.tb01195.x.

[25] J. Oksanen, F.G. Blanchet, M. Friendly, R. Kindt, P. Legendre, D. McGlinn, P.R. Minchin, R.B. O'hara, G.L. Simpson, P. Solymos, M.H.H. Stevens, E. Szoecs, H. Wagner, vegan: Community ecology package, (2018) 2.5-6.

[26] M.J. Anderson, K.E. Ellingsen, B.H. McArdle, Multivariate dispersion as a measure of beta diversity, Ecol. Lett. 9 (2006) 683–693. https://doi.org/10.1111/j.1461-0248.2006.00926.x.

[27] P.D. Karp, The MetaCyc Database, Nucleic Acids Res. (2002). https://doi.org/10.1093/nar/30.1.59.

[28] V.M. Markowitz, I.-M.A. Chen, K. Palaniappan, K. Chu, E. Szeto, Y. Grechkin, A. Ratner, B. Jacob, J. Huang, P. Williams, IMG: the integrated microbial genomes database and comparative analysis system, Nucleic Acids Res. 40 (2012) D115–D122.

[29] F. Rohart, B. Gautier, A. Singh, K.A. Lê Cao, mixOmics: An R package for 'omics feature selection and multiple data integration, PLoS Comput. Biol. 13 (2017) e1005752. https://doi.org/10.1371/journal.pcbi.1005752.

[30] A.D. Washburne, J.D. Silverman, J.T. Morton, D.J. Becker, D. Crowley, S. Mukherjee, L.A. David, R.K. Plowright, Phylofactorization: a graph partitioning algorithm to identify phylogenetic scales of ecological data, Ecol. Monogr. 89 (2019) e01353. https://doi.org/10.1002/ecm.1353.

[31] J.D. Rocca, M. Simonin, J.R. Blaszczak, J.G. Ernakovich, S.M. Gibbons, F.S. Midani, A.D. Washburne, The Microbiome Stress Project: Toward a global meta-analysis of environmental stressors and their effects on microbial communities, Front. Microbiol. 9 (2019) 3272. https://doi.org/10.3389/fmicb.2018.03272.

[32] Z.D. Kurtz, C.L. Müller, E.R. Miraldi, D.R. Littman, M.J. Blaser, R.A. Bonneau, Sparse and Compositionally Robust Inference of Microbial Ecological Networks, PLoS Comput. Biol. 11 (2015) e1004226. https://doi.org/10.1371/journal.pcbi.1004226.

[33] H. Liu, K. Roeder, L. Wasserman, Stability approach to regularization selection (StARS) for high dimensional graphical models, Adv. Neural Inf. Process. Syst. 24 (2010) 1432–1440.

[34] M. Bastian, S. Heymann, M. Jacomy, Gephi: an open source software for exploring and manipulating networks, Icwsm. 8 (2009) 361–362.

[35] V.D. Blondel, J.L. Guillaume, R. Lambiotte, E. Lefebvre, Fast unfolding of communities in large networks, J. Stat. Mech. Theory Exp. 10 (2008) P10008. https://doi.org/10.1088/1742-5468/2008/10/P10008.

[36] W.M. Post, J. Pastor, P.J. Zinke, A.G. Stangenberger, Global patterns of soil nitrogen storage, Nature. 317 (1985) 613–616. https://doi.org/10.1038/317613a0.

[37] J.A. Baldock, J. Sanderman, L.M. MacDonald, A. Puccini, B. Hawke, S. Szarvas, J. McGowan, Quantifying the allocation of soil organic carbon to biologically significant fractions, Soil Res. 51 (2013) 561–576. https://doi.org/10.1071/SR12374.

[38] X. Xiao, Z. Chen, B. Chen, H/C atomic ratio as a smart linkage between pyrolytic temperatures, aromatic clusters and sorption properties of biochars derived from diverse precursory materials, Sci. Rep. 6 (2016) 22644.

[39] J. Lehmann, M. Kleber, The contentious nature of soil organic matter, Nature. 528 (2015) 60–68.

[40] J.M. Lavallee, J.L. Soong, M.F. Cotrufo, Conceptualizing soil organic matter into particulate and mineral-associated forms to address global change in the 21st century, Glob. Chang. Biol. 26 (2020) 261–273. https://doi.org/10.1111/gcb.14859.

[41] J. Lehmann, C.M. Hansel, C. Kaiser, M. Kleber, K. Maher, S. Manzoni, N. Nunan, M. Reichstein, J.P. Schimel, M.S. Torn, W.R. Wieder, I. Kögel-Knabner, Persistence of soil organic carbon caused by functional complexity, Nat. Geosci. (2020) 1–6. https://doi.org/10.1038/s41561-020-0612-3.

[42] O. Pelz, W.R. Abraham, M. Saurer, R. Siegwolf, J. Zeyer, Microbial assimilation of plant-derived carbon in soil traced by isotope analysis, Biol. Fertil. Soils. 41 (2005) 153–162. https://doi.org/10.1007/s00374-004-0826-3.

[43] J.H. Brown, J.F. Gillooly, A.P. Allen, V.M. Savage, G.B. West, Toward a metabolic theory of ecology, Ecology. 85 (2004) 1771–1789. https://doi.org/10.1890/03-9000.

[44] W.J. Parton, The CENTURY model, in: Eval. Soil Org. Matter Model., 1996: pp. 283–291. https://doi.org/10.1007/978-3-642-61094-3_23.

[45] W.J. Parton, D.S. Schimel, C. V. Cole, D.S. Ojima, Analysis of Factors Controlling Soil Organic Matter Levels in Great Plains Grasslands, Soil Sci. Soc. Am. J. 51 (1987) 1173–1179. https://doi.org/10.2136/sssaj1987.03615995005100050015x.

[46] C. Chenu, D.A. Angers, P. Barré, D. Derrien, D. Arrouays, J. Balesdent, Increasing organic stocks in agricultural soils: Knowledge gaps and potential innovations, Soil Tillage Res. 188 (2019) 41–52. https://doi.org/10.1016/j.still.2018.04.011.

[47] D.A. Lipson, The complex relationship between microbial growth rate and yield and its implications for ecosystem processes, Front. Microbiol. 6 (2015) 615. https://doi.org/10.3389/fmicb.2015.00615.

[48] T. Fuhrer, E. Fischer, U. Sauer, Experimental identification and quantification of glucose metabolism in seven bacterial species, J. Bacteriol. 187 (2005) 1581–1590. https://doi.org/10.1128/JB.187.5.1581-1590.2005.

[49] A. Flamholz, E. Noor, A. Bar-Even, W. Liebermeister, R. Milo, Glycolytic strategy as a tradeoff between energy yield and protein cost, Proc. Natl. Acad. Sci. 110 (2013) 10039–10044. https://doi.org/10.1073/pnas.1215283110.

[50] L. Han, K. Sun, J. Jin, X. Wei, X. Xia, F. Wu, B. Gao, B. Xing, Role of structure and microporosity in phenanthrene sorption by natural and engineered organic matter, Environ. Sci. Technol. 48 (2014) 11227–11234. https://doi.org/10.1021/es5022087.

[51] A. Gunina, Y. Kuzyakov, Sugars in soil and sweets for microorganisms: Review of origin, content, composition and fate, Soil Biol. Biochem. 90 (2015) 87–100. https://doi.org/10.1016/j.soilbio.2015.07.021.

[52] P.T. Vanhooren, E.J. Vandamme, L-Fucose: Occurrence, physiological role, chemical, enzymatic and microbial synthesis, J. Chem. Technol. Biotechnol. 74 (1999) 479–497. https://doi.org/10.1002/(SICI)1097-4660(199906)74:6<479::AID-JCTB76>3.0.CO;2-E.

[53] R.M. Maier, G. Soberón-Chávez, Pseudomonas aeruginosa rhamnolipids: Biosynthesis and potential applications, Appl. Microbiol. Biotechnol. 54 (2000) 625–633. https://doi.org/10.1007/s002530000443.

[54] S. Spielvogel, J. Prietzel, I. Kögel-Knabner, Changes of lignin phenols and neutral sugars in different soil types of a high-elevation forest ecosystem 25 years after forest dieback, Soil Biol. Biochem. 39 (2007) 655–668. https://doi.org/10.1016/j.soilbio.2006.09.018.

[55] L.E. Lowe, Carbohydrates in soil, in: Dev. Soil Sci., Elsevier, 1978: pp. 65–93.

[56] J.S. Singh, A.S. Raghubanshi, R.S. Singh, S.C. Srivastava, Microbial biomass acts as a source of plant nutrients in dry tropical forest and savanna, Nature. 338 (1989) 499–500. https://doi.org/10.1038/338499a0.

[57] M. Hemkemeyer, B.T. Christensen, R. Martens, C.C. Tebbe, Soil particle size fractions harbour distinct microbial communities and differ in potential for microbial mineralisation of organic pollutants, Soil Biol. Biochem. 90 (2015) 255–265. https://doi.org/10.1016/j.soilbio.2015.08.018.

[58] A.D. Washburne, J.D. Silverman, J.W. Leff, D.J. Bennett, J.L. Darcy, S. Mukherjee, N. Fierer, L.A. David, Phylogenetic factorization of compositional data yields lineage-level associations in microbiome datasets, PeerJ. 5 (2017) e2969. https://doi.org/10.7717/peerj.2969.

[59] N.L. Ward, J.F. Challacombe, P.H. Janssen, B. Henrissat, P.M. Coutinho, M. Wu, G. Xie, D.H. Haft, M. Sait, J. Badger, R.D. Barabote, B. Bradley, T.S. Brettin, L.M. Brinkac, D. Bruce, T. Creasy, S.C. Daugherty, T.M. Davidsen, R.T. DeBoy, J.C. Detter, R.J. Dodson, A.S. Durkin, A. Ganapathy, M. Gwinn-Giglio, C.S. Han, H. Khouri, H. Kiss, S.P. Kothari, R. Madupu, K.E. Nelson, W.C. Nelson, I. Paulsen, K. Penn, Q. Ren, M.J. Rosovitz, J.D. Selengut, S. Shrivastava, S.A. Sullivan, R. Tapia, S. Thompson, K.L. Watkins, Q. Yang, C. Yu, N. Zafar, L. Zhou, C.R. Kuske, Three genomes from the

phylum Acidobacteria provide insight into the lifestyles of these microorganisms in soils, Appl. Environ. Microbiol. 74 (2009) 2046–2056. https://doi.org/10.1128/AEM.02294-08.

[60] F. Sakakibara, K. Takagi, R. Kataoka, H. Kiyota, Y. Sato, S. Okada, Isolation and identification of dieldrin-degrading Pseudonocardia sp. strain KSF27 using a soil–charcoal perfusion method with aldrin trans-diol as a structural analog of dieldrin, Biochem. Biophys. Res. Commun. 411 (2011) 76–81.

[61] A. Bajaj, S. Mayilraj, M.K.R. Mudiam, D.K. Patel, N. Manickam, Isolation and functional analysis of a glycolipid producing Rhodococcus sp. strain IITR03 with potential for degradation of 1,1,1-trichloro-2,2-bis(4-chlorophenyl)ethane (DDT), Bioresour. Technol. 167 (2014) 398–406. https://doi.org/10.1016/j.biortech.2014.06.007.

[62] H. Liu, C.F. Shen, K. Wang, Y.X. Chen, Cometabolic degradation of pentachlorophenol by Sphingobacterium multivorum, Zhongguo Huanjing Kexue/China Environ. Sci. 24 (2004) 294–298.

[63] H. Fang, B. Dong, H. Yan, F. Tang, Y. Yu, Characterization of a bacterial strain capable of degrading DDT congeners and its use in bioremediation of contaminated soil, J. Hazard. Mater. 184 (2010) 281–289.

[64] H. Fullerton, C.L. Moyer, Comparative single-cell genomics of Chloroflexi from the Okinawa Trough deep-subsurface biosphere, Appl. Environ. Microbiol. 82 (2016) 3000–3008. https://doi.org/10.1128/AEM.00624-16.

[65] K.T. Finneran, H.M. Forbush, C. V. Gaw VanPraagh, D.R. Lovley, Desulfitobacterium metallireducens sp. nov., an anaerobic bacterium that couples growth to the reduction of metals and humic acids as well as chlorinated compounds, Int. J. Syst. Evol. Microbiol. 41 (2002) 1929–1935. https://doi.org/10.1099/ijs.0.02121-0.

[66] M. Chen, H. Tong, C. Liu, D. Chen, F. Li, J. Qiao, A humic substance analogue AQDS stimulates Geobacter sp. abundance and enhances pentachlorophenol transformation in a paddy soil, Chemosphere. 160 (2016) 141–148. https://doi.org/10.1016/j.chemosphere.2016.06.061.

[67] F.P. Van der Zee, F.J. Cervantes, Impact and application of electron shuttles on the redox (bio)transformation of contaminants: A review, Biotechnol. Adv. 27 (2009) 256–277. https://doi.org/10.1016/j.biotechadv.2009.01.004.

[68] R. Boopathy, Factors limiting bioremediation technologies, Bioresour. Technol. 74 (2000) 63–67. https://doi.org/10.1016/S0960-8524(99)00144-3.

Figures

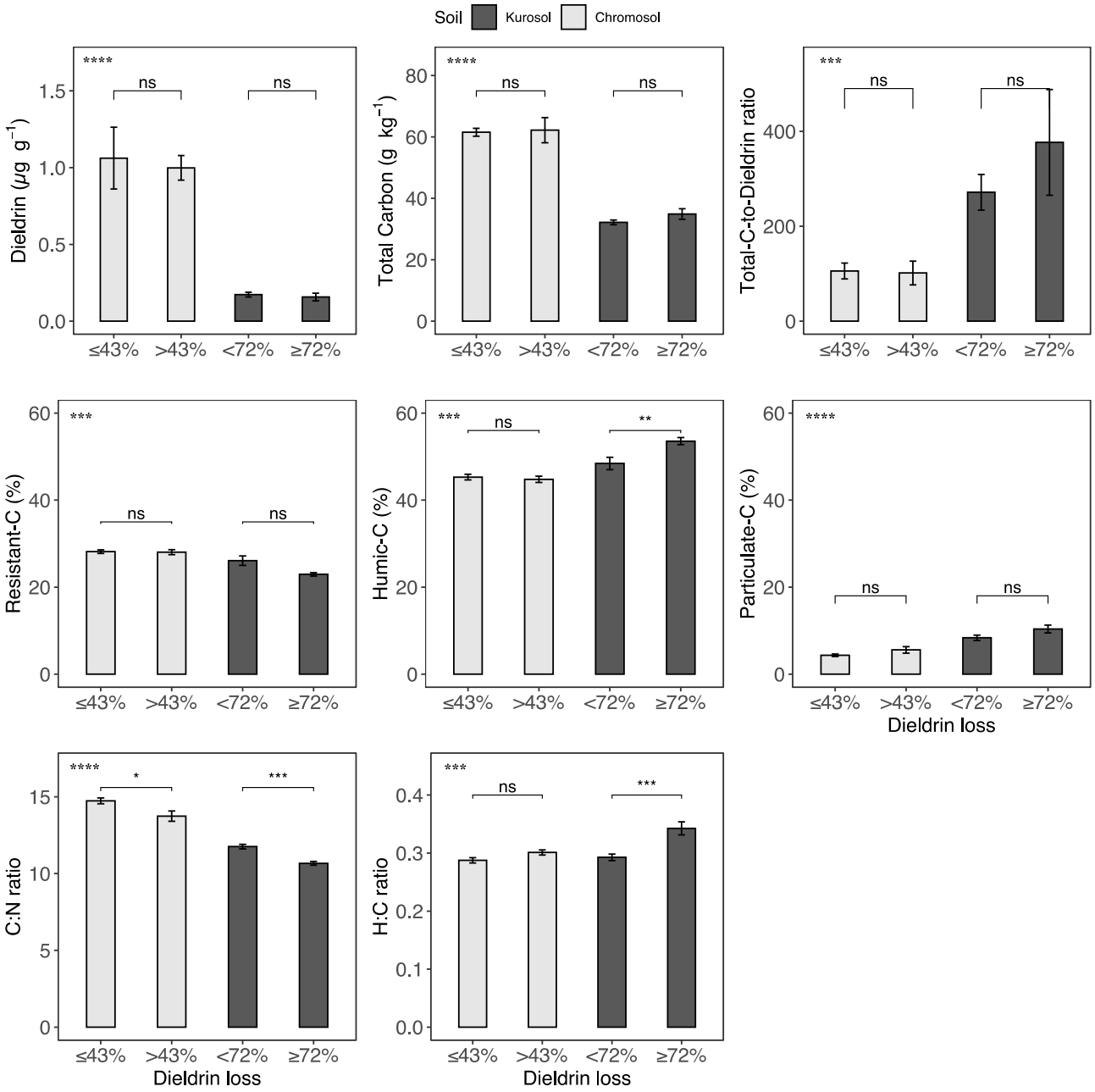

Figure 1. Comparisons of carbon quality variables between samples of low and high dieldrin losses. Samples are grouped into four categories (≤43 %, n = 9; >43 %, n = 6; <72 %, n = 9; ≥72 %, n = 12) based on long-term dieldrin loss (%) where the loss is either below or above the median dieldrin loss in each soil type (Median loss was 43% and 72% in the Chromosol and Kurosol, respectively). Predictions of resistant organic carbon (Resistant-C), humic carbon (Humic-C) and particulate organic carbon (Particulate-C) are shown as percentages to total organic carbon. Significance levels of global Kruskal-Wallis tests for dieldrin loss categories (top-left of each panel) and Wilcoxon tests (above each group) for each soil type are shown (ns > 0.05; * ≤ 0.05; ** ≤ 0.01; *** ≤ 0.001; **** ≤ 0.0001).

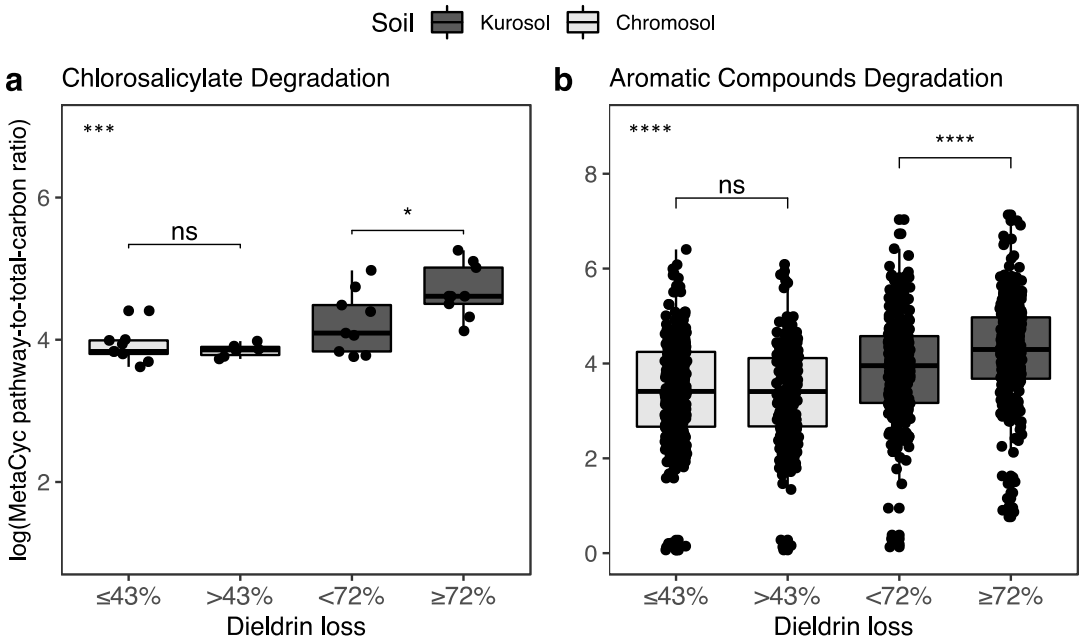

Figure 2. Comparison of degradation potentials of 1 chlorinated (a) and 39 aromatic compounds (b) predicted to be present in all samples (excluding outliers). Samples are grouped into four categories based on long-term dieldrin loss (≤43 %, n = 9; >43 %, n = 6; <72 %, n = 9; ≥72 %, n = 9) where the loss is either below or above the median dieldrin loss in each soil type (Median loss was 43% and 72% in the Chromosol and Kurosol, respectively). Significances of global Kruskal-Wallis tests for dieldrin loss categories (top-left of each panel) and Wilcoxon tests (above each group) for each soil type are shown (ns > 0.05; * ≤ 0.05; ** ≤ 0.01; *** ≤ 0.001; **** ≤ 0.0001).

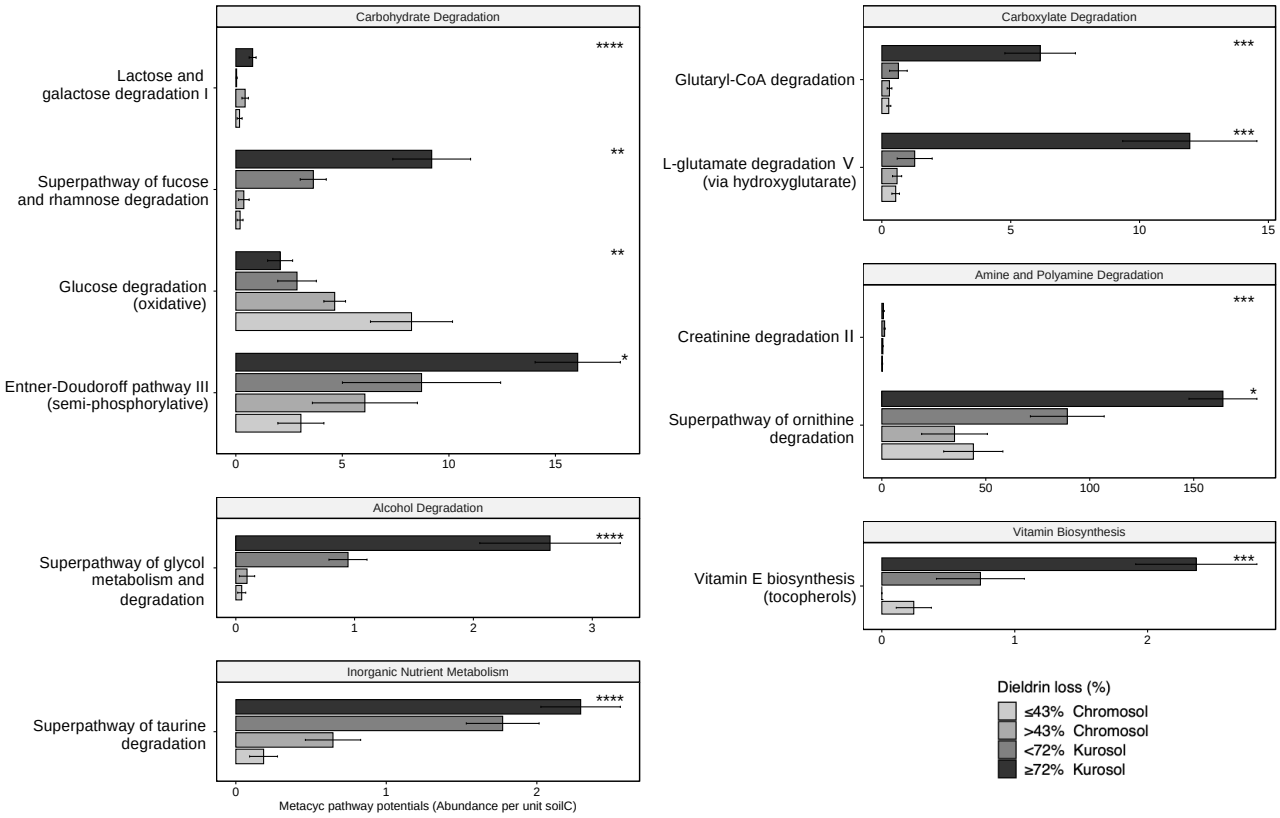

Figure 3. MetaCyc pathway potentials (Pathway abundances per g soil carbon) which were key predictors for dieldrin loss (%) in sparse-partial-least-squares analysis using the mixOmics package. Samples are grouped into four categories based on long-term dieldrin loss (≤43 %, n = 9; >43 %, n = 6; <72 %, n = 9; ≥72 %, n = 9) where the loss is either below or above the median dieldrin loss in each soil type (Median loss was 43% and 72% in the Chromosol and Kurosol, respectively). Significances of global Kruskal-Wallis tests (top-left) and Wilcoxon tests (above each group) for each soil type are shown (ns > 0.05; * ≤ 0.05; ** ≤ 0.01; *** ≤ 0.001; **** ≤ 0.0001).

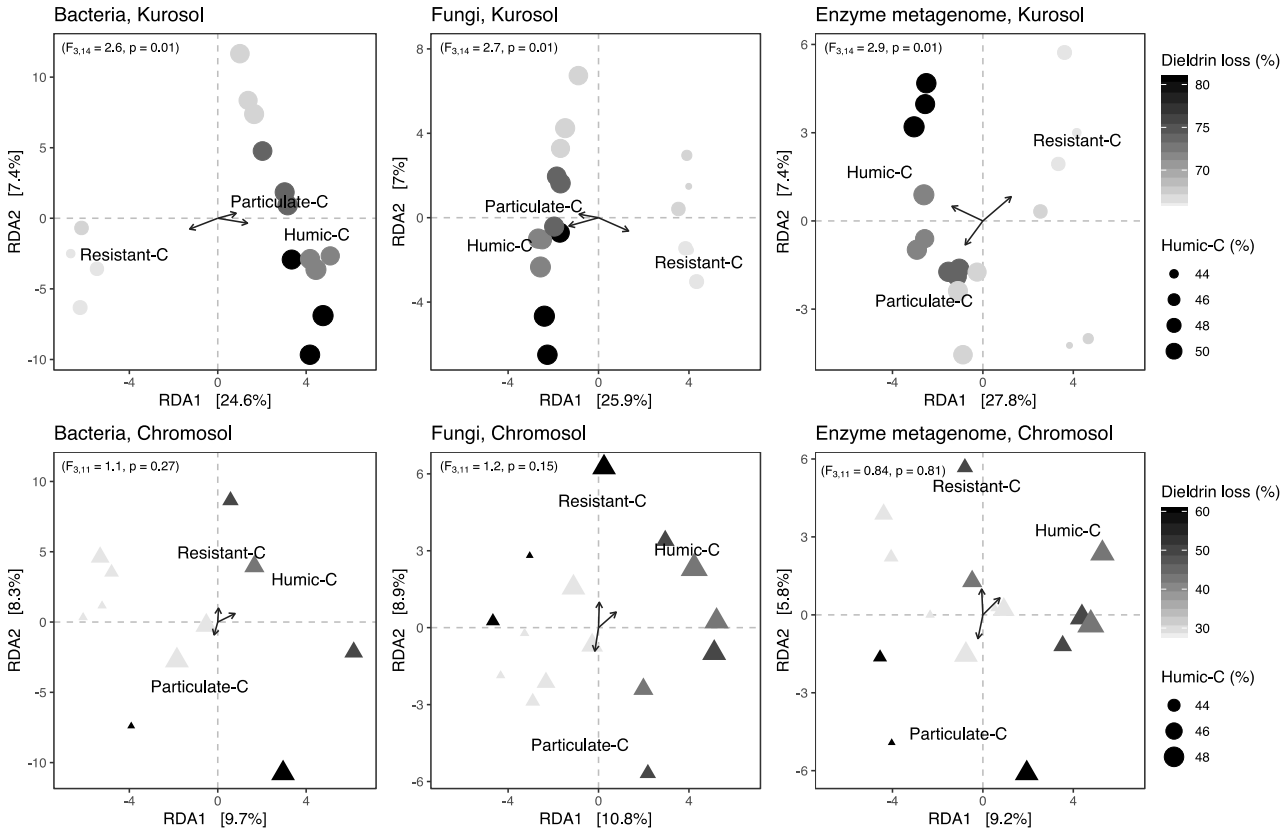

Figure 4. Redundancy analysis of bacterial and fungal abundances using the centered log-ratio transformed proportions of resistant organic carbon (Resistant-C), humic organic carbon (Humic-C) and particulate organic carbon (Particulate-C) as constraining variables. Symbols represent individual samples, and their proximity to each other indicates compositional similarity. The size and shape of symbols indicate the long-term dieldrin loss (%) of samples. Three samples from the Kurosol were removed as outliers (Kurosol, n = 18; Chromosol, n = 15).

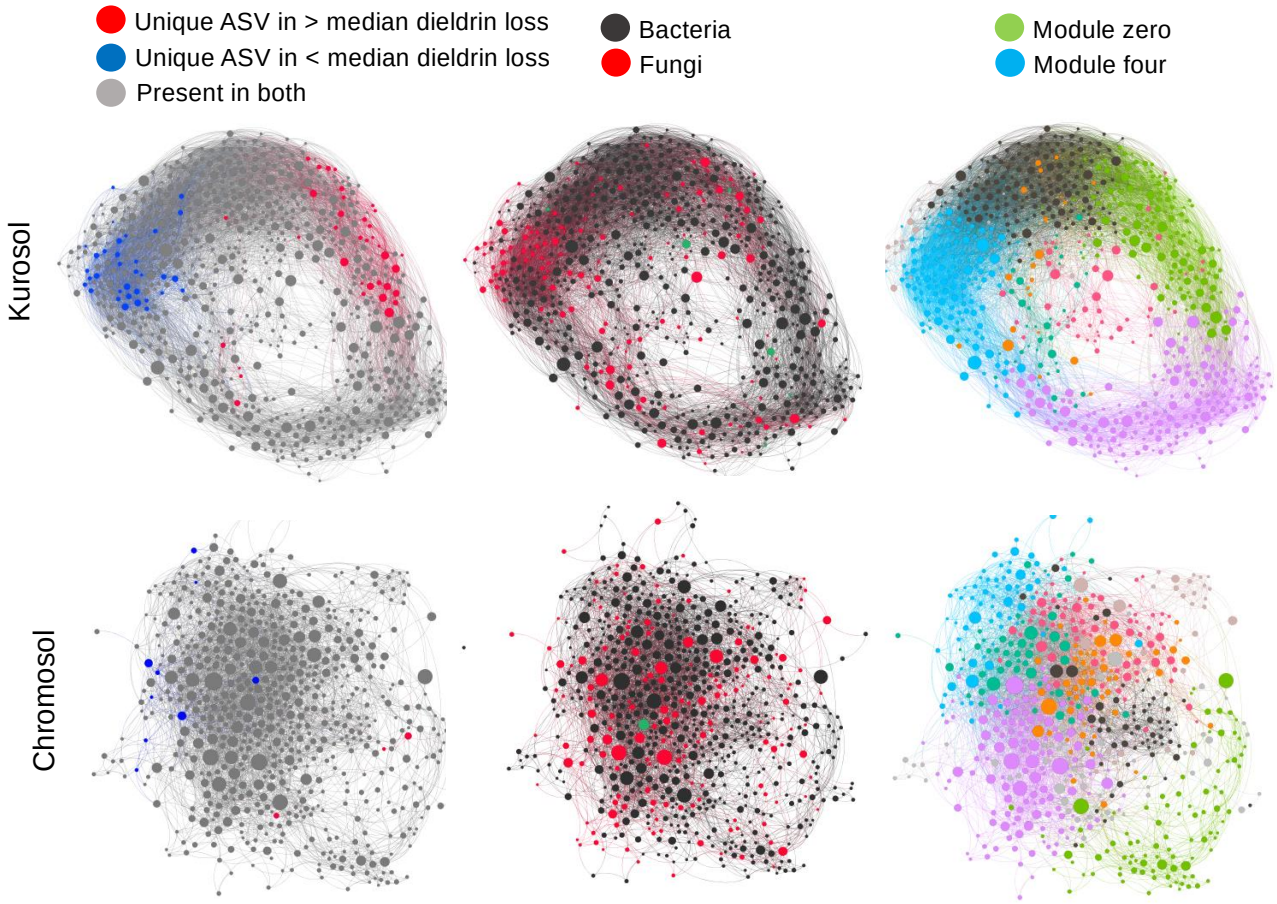

Figure 5. Co-occurrence network of fungi and bacteria in the Kurosol and the Chromosol using the SpiecEasi package (glasso) and modified in gephi. Edge lengths are proportional to distance between nodes (Force Atlas). Size of nodes indicate Betweenness Centrality. **Left**: Nodes highlight ASVs which were unique in sample groups with above or below median dieldrin loss (Median dieldrin loss was 43% and 72% in the Chromosol and Kurosol, respectively); **Middle**: Nodes are shown as either bacteria (dark grey) or fungi (Red); **Right**: Nodes are colored by modules that cluster together non-randomly (gephi modularity). The combined abundance of module zero in the Kurosol correlated with concentrations of humic carbon ($R^2 = 0.57$, $p<0.001$). Three samples from the Kurosol were removed as outliers (Kurosol, n = 18; Chromosol, n = 15).

Table 1. Top correlation coefficients between dieldrin loss and soil resistant organic carbon (ROC), humic organic carbon (HOC) and particulate organic carbon (POC) and carbon-to-nitrogen ratio (C/N) obtained from component loadings of sparse-partial-least-squares analysis in regression mode.

Metacyc Pathway	Dieldrin loss[a]	ROC	HOC	POC	C/N
Sparse partial least squares model for Chromosol and Kurosol samples (n = 33)					
3-phenylpropanoate degradation	**-0.89**	0.77	-0.42	-0.78	0.90
4-aminobutanoate degradation V	**-0.87**	0.76	-0.47	-0.75	0.87
Homolactic fermentation	**-0.85**	0.77	-0.55	-0.72	0.86
Protocatechuate degradation II (ortho-cleavage pathway)	**-0.85**	0.71	-0.29	-0.76	0.86
Aromatic biogenic amine degradation (bacteria)	**-0.85**	0.73	-0.36	-0.75	0.86
Superpathway of fucose and rhamnose degradation	**0.88**	-0.74	0.33	0.78	-0.89
Superpathway of glycol metabolism and degradation	**0.88**	-0.74	0.34	0.78	-0.89
Sparse partial least squares model for Kurosol samples (n = 18)[b]					
Ubiquinol-8 biosynthesis (prokaryotic)	**-0.86**	0.47	-0.81	-0.21	0.73
tRNA processing	**-0.86**	0.50	-0.82	-0.23	0.73
Superpathway of ubiquinol-8 biosynthesis (prokaryotic)	**-0.86**	0.47	-0.81	-0.21	0.73
Inosine 5'-phosphate degradation	**-0.85**	0.56	-0.84	-0.28	0.72
Superpathway of b heme biosynthesis from glycine	**-0.85**	0.64	-0.86	-0.35	0.71
Superpathway of L-phenylalanine biosynthesis	**-0.85**	0.47	-0.81	-0.21	0.73
Superpathway of L-tyrosine biosynthesis	**-0.85**	0.47	-0.81	-0.21	0.73
Superpathway of heme-b biosynthesis from uroporphyrinogen-III	**-0.85**	0.63	-0.85	-0.34	0.71
Lactose and galactose degradation I	**0.80**	-0.70	0.84	0.41	-0.66
L-arginine degradation (Stickland reaction)	**0.83**	-0.62	0.83	0.33	-0.69

[a] Only top variable coefficients to dieldrin loss are shown ($R \leq -0.85$ or ≥ 0.80).
[b] Coefficients for separate model of Chromosol samples (n = 15) were not significant and therefore not shown.

Table 2. Results of 999 permutations of a pseudo-F statistic on constraining variables resistant organic carbon (Resistant-C), humic organic carbon (Humic-C) and particulate organic carbon (Particulate-C).

	Kurosol				Chromosol			
Carbon Fraction	**df**	**Variance**	**pseudoF**	***p***	**df**	**Variance**	**pseudoF**	***p***
Bacteria								
Humic-C	1	980	2.65	**0.01**	1	528	1.34	0.11
Particulate-C	1	470	1.27	0.17	1	292	0.74	0.93
Resistant-C	1	576	1.56	0.09	1	310	0.79	0.85
Residual	14	5183			14	4345		
Fungi								
Humic-C	1	117	2.36	**0.01**	1	93	1.49	0.06
Particulate-C	1	60	1.21	0.19	1	45	0.72	0.96
Resistant-C	1	79	1.6	0.07	1	50	0.80	0.83
Residual	14	692			14	687		
Enzyme-encoding genes								
Humic-C	1	124	2.99	**<0.01**	1	70	1.03	0.35
Particulate-C	1	40	0.96	0.44	1	34	0.49	1.00
Resistant-C	1	54	1.3	0.18	1	46	0.69	0.92
Residual	14	582			14	745		

Carbon fractions were centered log-ratio transformed before analysis. Kurosol, n = 18; Chromosol, n = 15

Table 3. Richness of taxonomic groups which had a significantly higher chance of presence in samples with high dieldrin dissipation.

Phylum	Class	Order	≤43%[c]	>43%[c]	<72%[c]	≥72%[c]	Total ASVs
Acidobacteria Total (29-member Monophyletic clade)[a]			**24**	**17**	**51**	**129**	**221**
Acidobacteria	Acidobacteriia	Acidobacteriales[d]	24	17	51	129	221
Actinobacteria Total (18-member Monophyletic clade)[a]			**7**	**7**	**51**	**68**	**133**
Actinobacteria	Thermoleophilia	Solirubrobacterales	7	7	51	68	133
Bacteroidetes Total (17-member Monophyletic clade)[a]			**3**	**2**	**7**	**42**	**54**
Bacteroidetes	Unknown	Unknown	0	0	3	0	3
Bacteroidetes	Cytophagia	Cytophagales	1	0	2	3	6
Bacteroidetes	Sphingobacteriia	Sphingobacteriales	2	2	2	4	10
Bacteroidetes	Bacteroidia	Bacteroidales	0	0	0	35	35
Chloroflexi Total (6-member Monophyletic clade)[a]			**0**	**0**	**2**	**31**	**33**
Chloroflexi	Ktedonobacteria	TK10	0	0	0	5	5
Chloroflexi	Anaerolineae	WCHB1-50	0	0	2	26	28
Planctomycetes Total (17-member Monophyletic clade)[a]			**4**	**2**	**20**	**67**	**93**
Planctomycetes	Planctomycetia	Gemmatales	4	2	20	67	93
Actinobacteria Total (589-member Monophyletic clade)[b]			**977**	**683**	**1171**	**1831**	**4662**
Actinobacteria	Actinobacteria		0	0	0	1	1
Actinobacteria	MB-A2-108	0319-7L14	0	8	9	7	24
Actinobacteria	Thermoleophilia	Gaiellales	221	168	311	385	1085
Actinobacteria	Thermoleophilia	Solirubrobacterales	213	141	255	406	1015
Actinobacteria	Actinobacteria	Actinomycetales	543	366	596	1032	2537
Bacteroidetes Total (55-member Monophyletic clade)[b]			**7**	**8**	**12**	**153**	**180**
Bacteroidetes	Unknown	Unknown	0	0	3	0	3
Bacteroidetes	Cytophagia	Cytophagales	1	0	2	3	6
Bacteroidetes	Sphingobacteriia	Sphingobacteriales	3	3	5	9	20
Bacteroidetes	Bacteroidia	Bacteroidales	3	5	2	141	151
Chloroflexi Total (27-member Monophyletic clade)[b]			**10**	**14**	**23**	**94**	**141**
Chloroflexi	C0119	Unknown	3	2		3	8
Chloroflexi	Anaerolineae	H39	7	8	10	10	35
Chloroflexi	Ktedonobacteria	TK10	0	4	9	19	32
Chloroflexi	Anaerolineae	WCHB1-50	0	0	2	26	28
Chloroflexi	Anaerolineae	Anaerolineales	0	0	2	36	38
Firmicutes Total (44-member Monophyletic clade)[b]			**30**	**19**	**20**	**129**	**198**
Firmicutes	Clostridia	Thermoanaerobacterales	0	0	0	3	3
Firmicutes	Erysipelotrichi	Erysipelotrichales	0	0	0	6	6
Firmicutes	Clostridia	Clostridiales	30	19	20	120	189
Proteobacteria Total (24-member Monophyletic clade)[b]			**10**	**14**	**24**	**97**	**145**
Proteobacteria	Deltaproteobacteria	Desulfuromonadales[e]	10	14	24	97	145

[a] Phylofactors for Chromosol and Kurosol samples (n = 33) representing taxonomic clades which had a significantly higher probability to be present in samples with above-median dieldrin loss. Aggregated presence of clades was significant (Table S4).
[b] Phylofactors model included Kurosol samples only (n = 18). Aggregated presence of all clades was significant (Table S4).
[c] ASV frequencies are grouped into four categories based on long-term dieldrin loss (%) where the loss is either below or above the median dieldrin loss in each soil type (Median loss was 43% and 72% in the Chromosol and Kurosol, respectively).
[d] The phylofactor clade of order Acidobacteriales comprised almost exclusively of the genus *Candidatus Koribacter*
[e] The phylofactor clade of order Desulfuromonadales comprised exclusively of the genus *Geobacter sp.*

Supplementary Materials

Decomposed organic carbon mediates the assembly of soil communities with traits for the biodegradation of chlorinated pollutants

By Christian Krohn et al.

Detailed description of modelling approach for sparse partial least squares analysis (sPLS) and sPLS discriminant analysis (sPLS-DA)

For sPLS, the predictor matrix (X) was composed of predicted pathway potentials which were filtered to those present in at least 50% of samples resulting in a total of 410 pathways. This was followed by centered log-ratio transformations to account for compositionality of the data (Pawlowsky-Glahn et al., 2015). Matrix Y, the response matrix, was composed of resistant-C, humic-C, particulate-C, C:N and dieldrin loss (%) where the carbon fractions were also centered log-ratio transformed. The analysis was done in regression mode and the first two components were selected for analysis as they had sufficient predictive power based on the Q^2 cutoff of 0.0975 (Lê Cao et al., 2008; Tenehaus, 1998). A heatmap with Ward clustering from the mixOmics package was used to display pair-wise associations between pathways and soil variables from the two components (Rohart et al., 2017).

Additionally, we performed the supervised sPLS discriminant analysis (sPLS-DA) to select pathways that most predicted long-term dieldrin losses (Lê Cao et al., 2011). Samples were grouped into factors that were below and above the median dieldrin loss (%) of each soil, with a total of four factors representing “low” and “high” dieldrin loss in the Chromosol and Kurosol. After cross-validation based on the Balanced Error Rate (Rohart et al., 2017), the first three components were selected with 70, 100 and 90 pathways, respectively. Kruskal-Wallis tests were done to test significant differences of mean abundances of metabolic pathways that contributed most to the three sPLS-DA components.

Lê Cao, K.A., Boitard, S., Besse, P., 2011. Sparse PLS discriminant analysis: Biologically relevant feature selection and graphical displays for multiclass problems. BMC Bioinformatics. https://doi.org/10.1186/1471-2105-12-253

Lê Cao, K.A., Rossouw, D., Robert-Granié, C., Besse, P., 2008. A sparse PLS for variable selection when integrating omics data. Stat. Appl. Genet. Mol. Biol. https://doi.org/10.2202/1544-6115.1390

Pawlowsky-Glahn, V., Egozcue, J.J., Tolosana-Delgado, R., 2015. Modeling and Analysis of Compositional Data, Modeling and Analysis of Compositional Data. https://doi.org/10.1002/9781119003144

Rohart, F., Gautier, B., Singh, A., Lê Cao, K.A., 2017. mixOmics: An R package for ‘omics feature selection and multiple data integration. PLoS Comput. Biol. https://doi.org/10.1371/journal.pcbi.1005752

Tenehaus, M., 1998. La Régression PLS: Théorie et Pratique. Éditons Technip, Paris.

Supplementary Figures

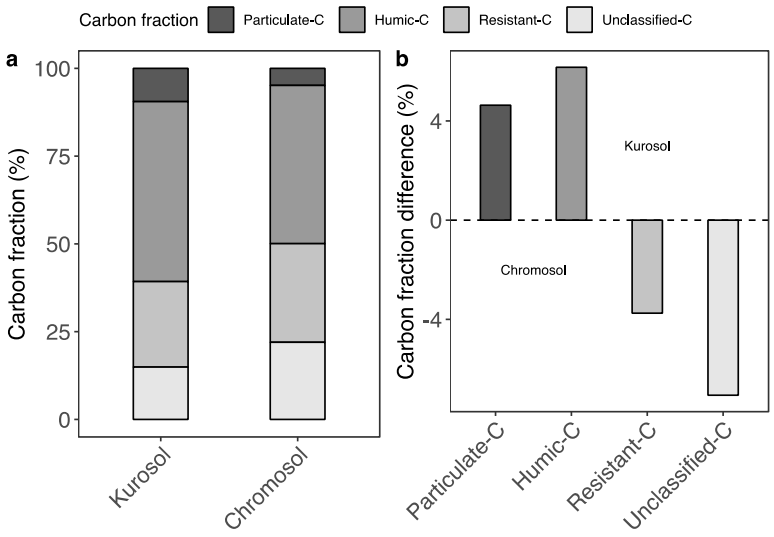

Figure S1. Comparisons of carbon fractions between Chromosol and Kurosol. Proportions of carbon (Particulate-C), humic organic carbon (Humic-C) and resistant organic carbon (Resistant-C) are shown by soil (a) and as the percent-difference of the Kurosol to the Chromosol (b). The residuals of prediction are denoted as 'Unclassified-C'.

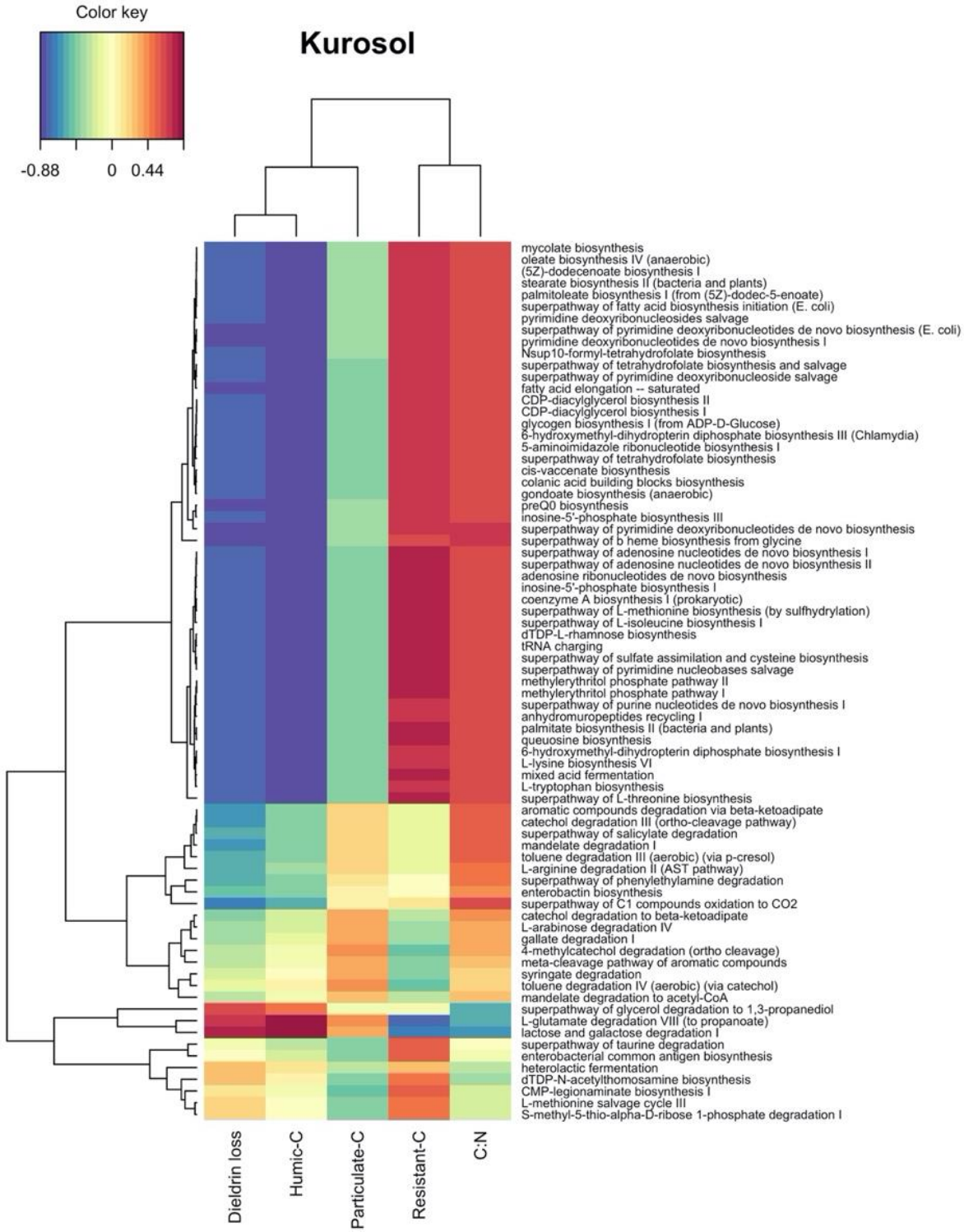

Figure S2. Ward clustered heatmap of similarity scores obtained from sparse partial least squares analysis in regression mode (R package mixOmics) for pathway potentials (rows) and soil variables (columns) for Kurosol samples. Soil variables included the long-term dieldrin loss (%), carbon-to-nitrogen ratios (C:N) and concentrations of resistant organic carbon (Resistant-C), humic carbon (Humic-C) and particulate organic carbon (Particulate-C). The pathway potentials and resistant-C, humic-C and particulate-C were centered log-ratio transformed before analysis.

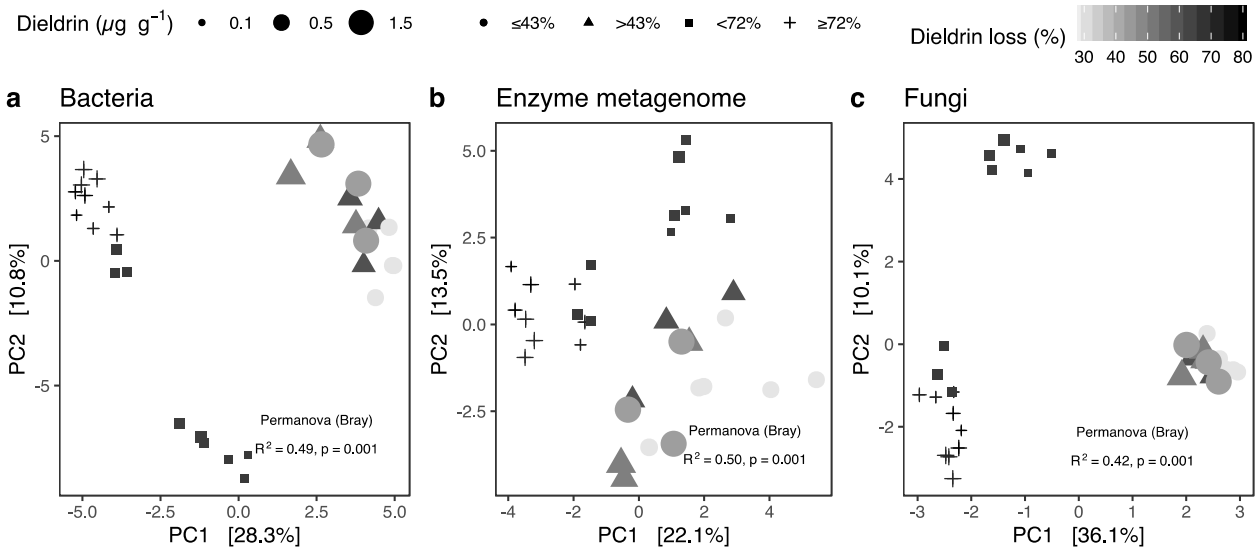

Figure S3. Ordinations of Aitchison distances were compared for compositions of bacteria, its enzyme metagenome as predicted by Picrust2 and fungi (n = 33). ASVs were filtered to those present in at least 25% of samples and included 1407 and 322 bacterial and fungal taxa, respectively, and 2091 enzyme encoding genes. Permanova results based on Bray-Curtis dissimilarities are shown. Symbols represent individual samples, and their proximity to each other indicates compositional similarity. The colour and size of symbols indicate the long-term dieldrin loss (%) and dieldrin concentrations, respectively. The shape of symbols indicates sample grouping into four factors where the loss is either below or above the median dieldrin loss in each soil type (Median loss was 43% and 72% in the Chromosol and Kurosol, respectively).

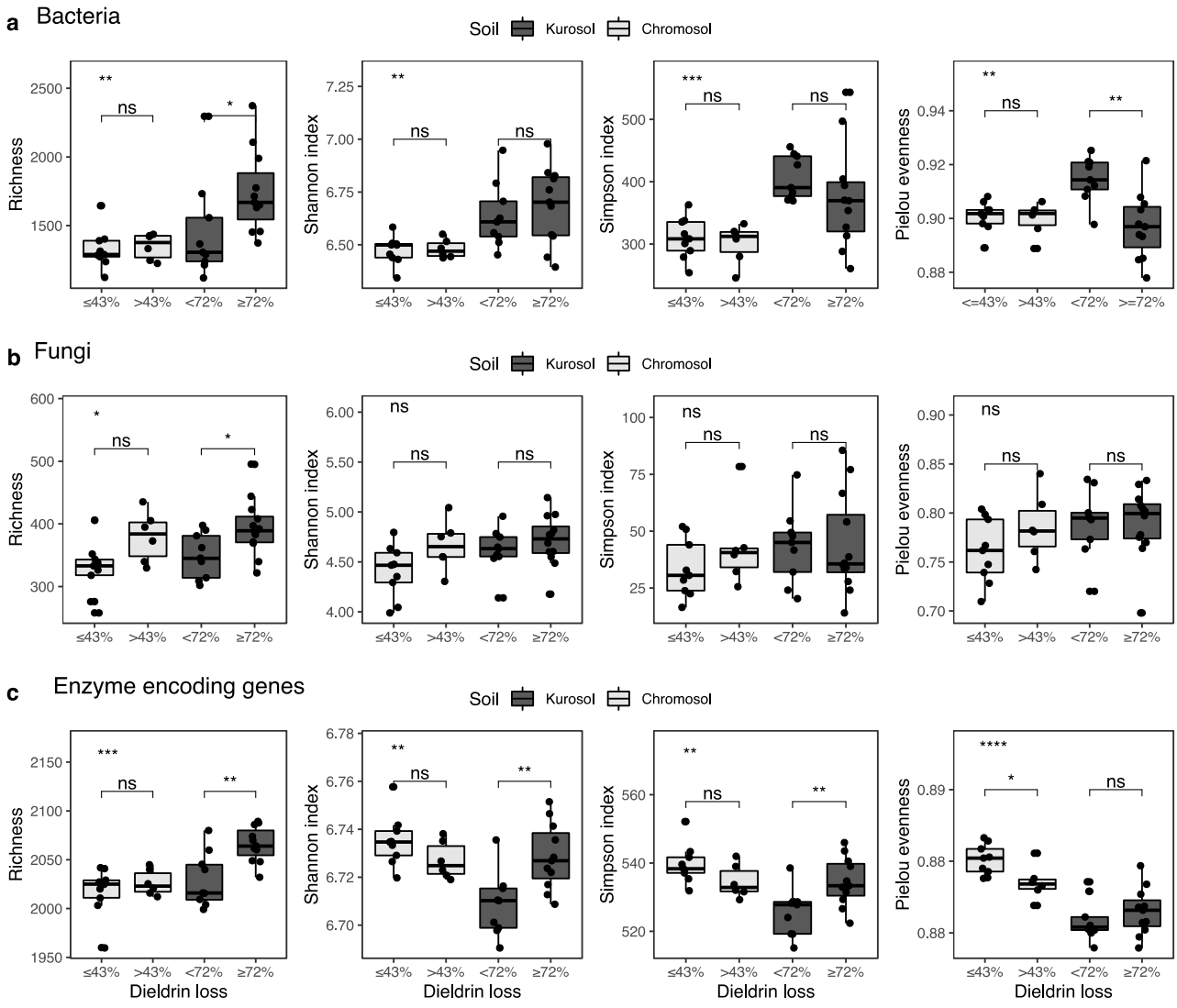

Figure S4. Alpha diversity of bacteria, fungi and the enzyme metagenome as predicted with Picrust2. Diversity indices were calculated from rarefied abundance of filtered amplicon sequence variants (ASVs) or enzyme abundances. Samples are grouped into four categories by long-term dielrin loss (%) where the loss is either below or above the median dieldrin loss in each soil type (Median loss was 43% and 72% in the Chromosol and Kurosol, respectively). Significance of global Kruskal-Wallis tests for dieldrin loss categories and Wilcoxon tests for each soil type are shown (ns, *, **, *** and **** represent p values of > 0.05, ≤0.05, ≤ 0.01, ≤ 0.001 and ≤ 0.0001, respectively).

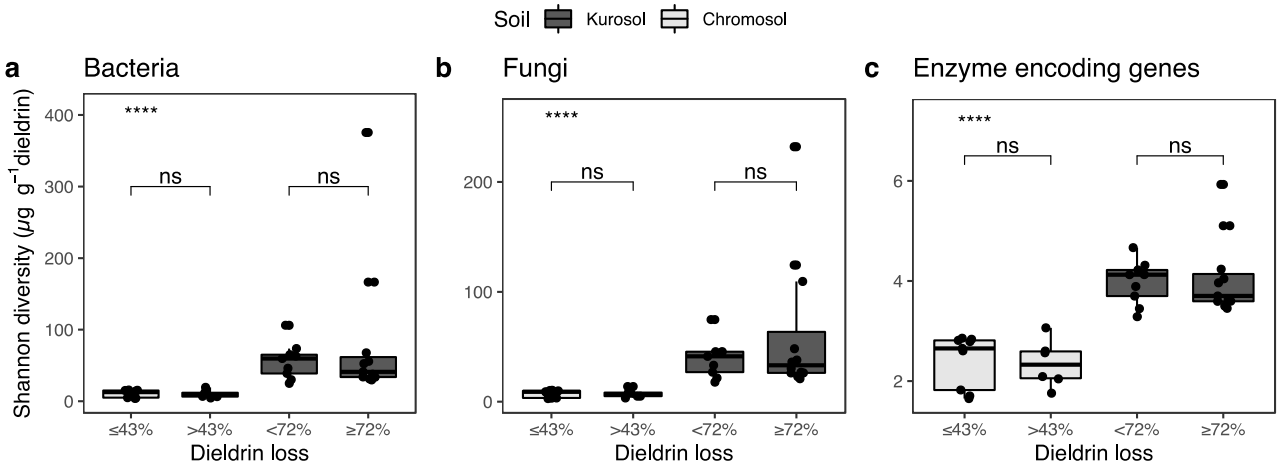

Figure S5. Shannon:dieldrin ratio of bacteria (a), fungi (b) and the enzyme metagenome as predicted from Picrust2 (c) per unit dieldrin (μg g^{-1}). Samples are grouped into four categories by long-term dieldrin loss (%) where the loss is either below or above the median dieldrin loss in each soil type (Median loss was 43% and 72% in the Chromosol and Kurosol, respectively). Significance of global Kruskal-Wallis tests for dieldrin loss categories and Wilcoxon tests for each soil type are shown (ns, $p > 0.05$; **** $p \leq 0.0001$).

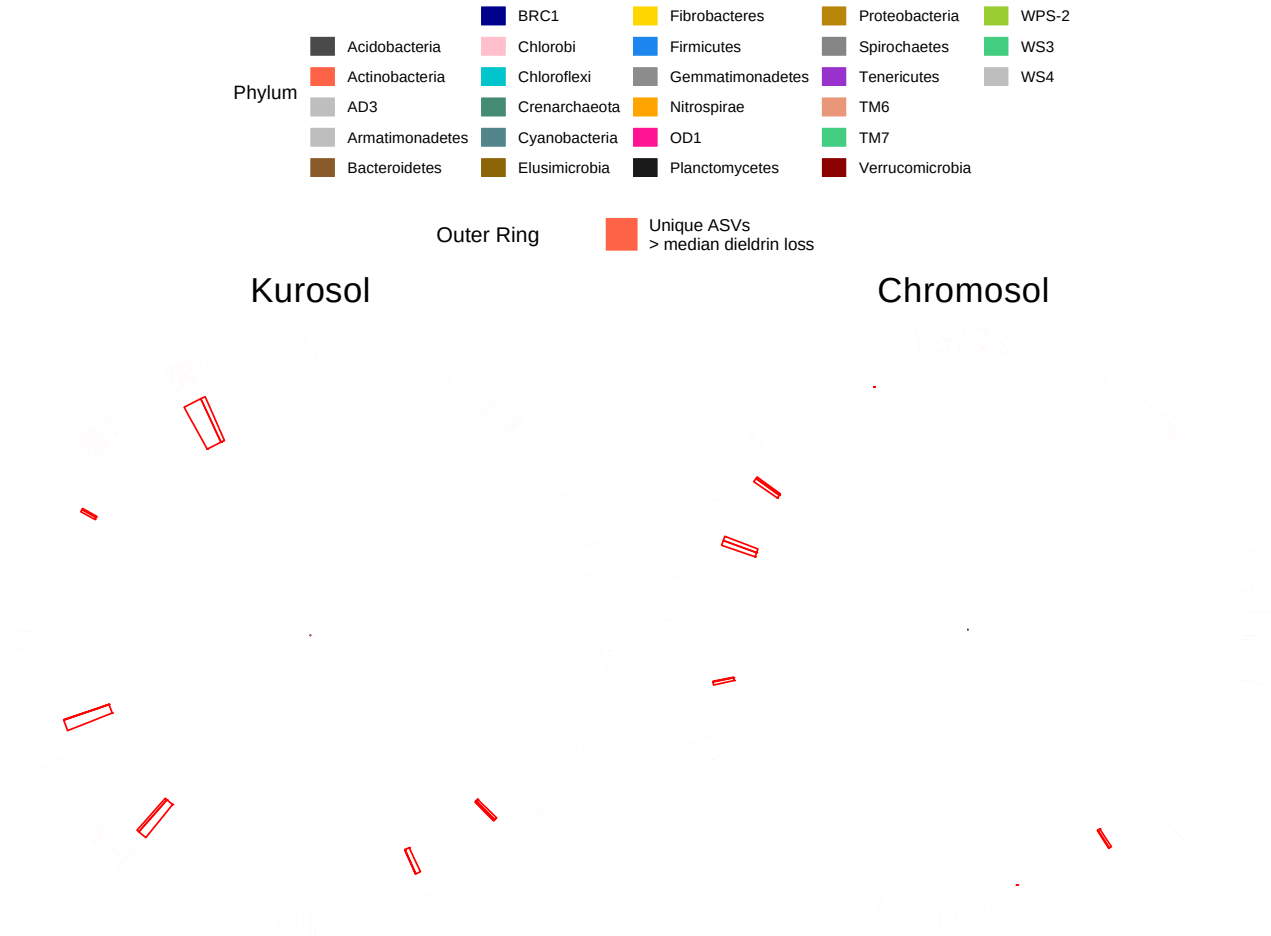

Figure S6. Soil comparison of phylogeny of all amplicon sequence variants (ASVs) present. Tips represent individual ASVs, and different colours indicate their phylum membership. Unique ASVs are shown in the outer ring where red indicates if ASVs were unique to a soil environment with above median dieldrin loss (%). On average 48 (Kurosol) or 21 (Chromosol) ASVs were unique in samples with above median dieldrin loss. Three outlier samples were removed prior to analysis (Kurosol, n = 18; Chromosol, n = 15). Polygons highlight phylogenetic clades with a higher chance of presence in 'high-dieldrin-loss' samples than could be explained by chance.

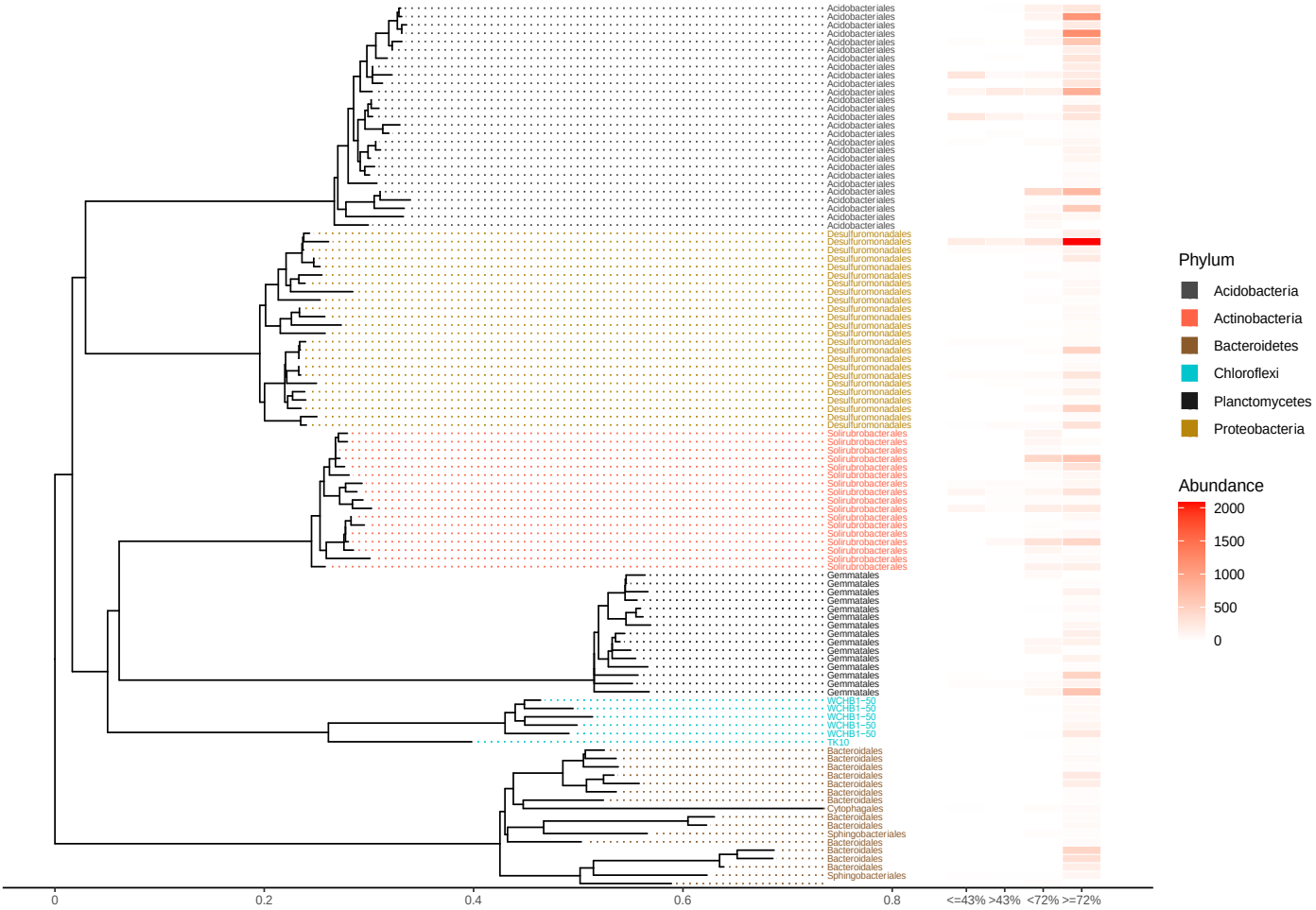

Figure S7. Phylogenetic clades with a higher chance of occurrence in 'high-dieldrin-loss' samples than could be explained by chance (Phylofactor generalised linear model with presence/absence as response variable). Samples are grouped into four categories based on long-term dieldrin loss (%) where the loss is either below or above the median dieldrin loss in each soil type (Median loss was 43% and 72% in the Chromosol and Kurosol, respectively). Prior to analysis, ASVs were filtered to those with a minimum of 10 reads. The phylofactor clade of order Desulfuromonadales comprised exclusively of the genus *Geobacter sp.*

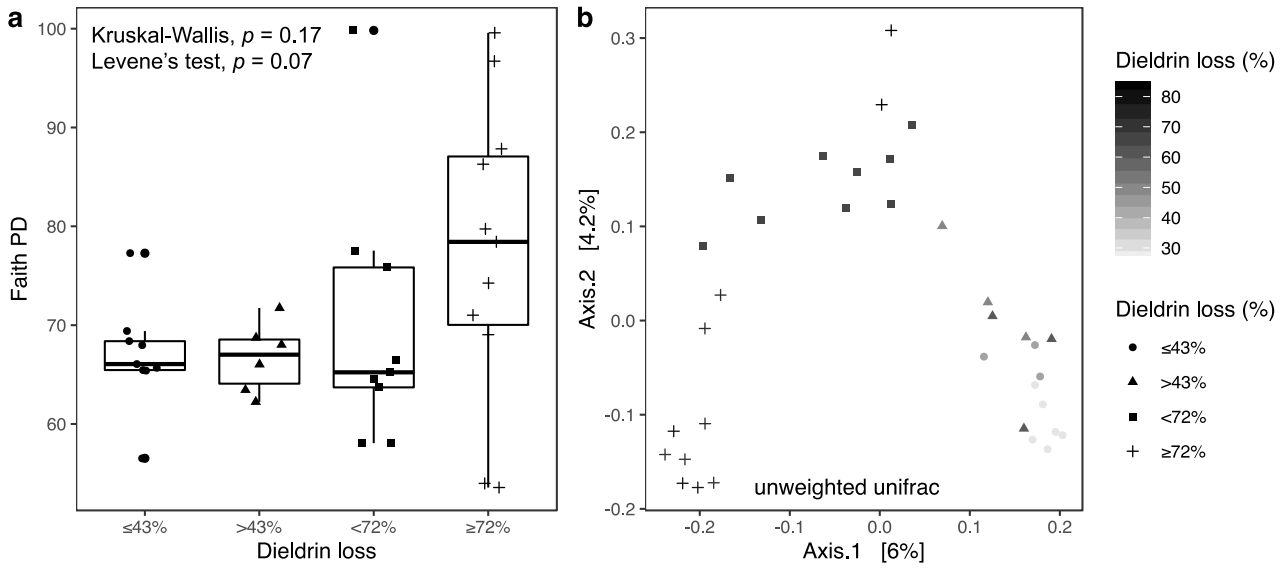

Figure S8. Faith phylogenetic diversity (Faith PD) index (a) and principle coordinate analysis (PCoA) with unweighted unifrac distances (b). Samples are grouped by long-term dieldrin loss (%) where the loss is either below or above the median loss in each soil type.

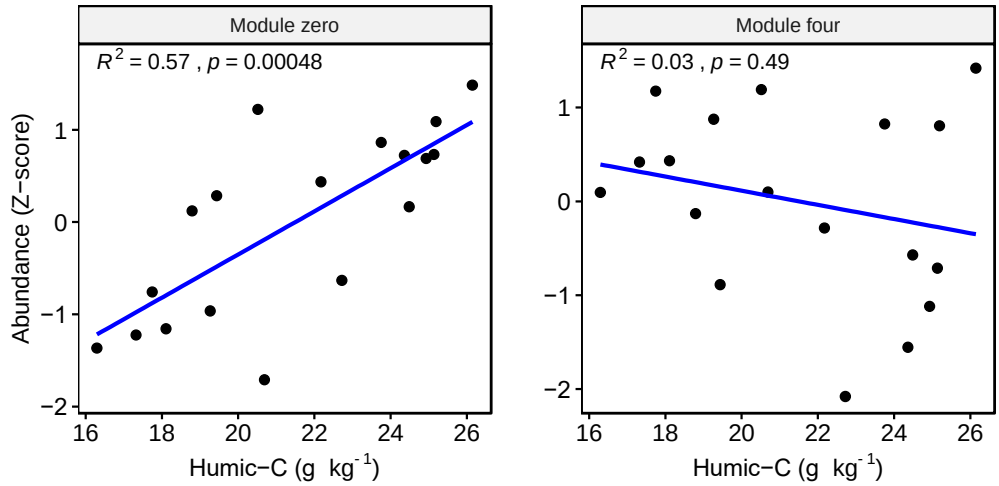

Figure S9. Scatter-plot of humic organic carbon concentration (Humic-C) and normalised abundances of the combined taxa in module zero and four from the network analysis of the Kurosol.

Supplementary Tables

Table S1. Climate data accessed from the Bureau of Meteorology on 22 May 2020.

Temperature (C°)

Northeast Victoria, King Valley, Edi upper, 1985 - 2020 (7 km to Kurosol paddocks)

Statistic	Jan	Feb	Mar	Apr	May	Jun	Jul	Aug	Sep	Oct	Nov	Dec	Annual	Mean Min Max
Mean	30.4	29.8	26.6	21.4	16.5	13.3	12	13.3	16.3	20.3	24	27.6	21	
Lowest	26.4	24.3	22.8	17.3	15	11.3	9.4	10.7	12.9	17.3	19.6	23	19	
Median	30.3	30.4	26.7	21.1	16.5	13.2	12.1	13.4	16.4	20.1	23.8	28.1	21	
Highest	35.3	33.9	30.3	25.7	18.9	15.2	14.6	15.7	18.6	25.1	29.9	32.4	22.4	
Min Max range	8.9	9.6	7.5	8.4	3.9	3.9	5.2	5	5.7	7.8	10.3	9.4	3.4	7.1
Southeast Victoria, Ferny Creek, 2011 - 2020 (15 km to Chromosol paddocks)														
Mean	24.5	24	21.1	17	13	10.4	9.8	10.8	13.9	17.2	19.2	22.3	17	
Lowest	22.4	21.5	17.6	15	11.1	9.7	8.5	9.2	12.7	15	17.5	20.6	16.3	
Median	24	24.4	22	16.8	13.2	10.3	9.7	10.5	13.7	17.2	19.5	21.9	17.2	
Highest	27.8	26.2	24	19.2	14.5	10.9	11.2	12.6	15.4	21.1	22.3	25.6	17.4	
Min Max range	5.4	4.7	6.4	4.2	3.4	1.2	2.7	3.4	2.7	6.1	4.8	5	1.1	4.2
Southeast Victoria, Scoresby Research institute, 1948 - 2020 (23 km to Chromosol paddocks)														
Mean	26.4	26.5	24.2	20.1	16.4	13.6	13.1	14.2	16.6	19.2	21.6	24.2	19.7	
Lowest	21.7	22.9	20.5	16.2	13.9	11.2	11.4	11.8	13.3	16.3	19.3	20.5	17.7	
Median	26.5	26.5	24.1	20.1	16.4	13.6	13	14.2	16.6	19	21.4	24.1	19.6	
Highest	31.6	31.2	27.8	23.6	18.8	15.7	15	16.8	19.1	24.7	26.5	29.3	21.2	
Min Max range	9.9	8.3	7.3	7.4	4.9	4.5	3.6	5	5.8	8.4	7.2	8.8	3.5	6.8

Rainfall (mm)

Northeast Victoria, King Valley, Edi upper, 1985 - 2020 (7 km to Kurosol paddocks)

Statistic	Jan	Feb	Mar	Apr	May	Jun	Jul	Aug	Sep	Oct	Nov	Dec	Annual	Mean Min Max
Mean	61	57	59	57	93	114	128	119	97	77	81	79	1029	
Lowest	3	3	1	6	11	15	39	14	24	4	23	2	364	
Median	45	34	47	37	76	109	125	116	84	57	72	76	982	
Highest	204	244	224	161	208	206	247	206	201	341	173	205	1606	
Min Max range	202	241	223	155	197	190	208	192	176	337	151	203	1242	206
Southeast Victoria, Beaconsfield upper, 1968 - 2020 (8.4 km to Chromosol paddocks)														
Mean	66	62	70	81	89	88	89	96	98	99	92	81	1016	
Lowest	3	0	14	20	16	17	27	35	44	33	0	0	589	
Median	66	44	64	70	91	84	81	96	85	97	94	80	1030	
Highest	152	237	234	192	191	180	200	162	209	214	201	206	1324	
Min Max range	149	237	221	172	175	162	173	127	165	181	201	206	735	181

Solar exposure (MJ m^{-2})

Northeast Victoria, King Valley, Edi Upper (Schmidts Farm Repeater), 1990 - 2020 (3.5 km to Kurosol paddocks)

Statistic	Jan	Feb	Mar	Apr	May	Jun	Jul	Aug	Sep	Oct	Nov	Dec	Annual	Mean Min Max
Mean	26.8	23.2	19	13.1	8.8	6.6	7.1	10.2	14.6	20.3	23.8	26.6	16.7	
Lowest	21.9	20.4	16.3	9.2	7.3	4.5	5.2	7	12.1	18.3	19.5	22.1	15.5	

Highest	31	26.6	21.8	15.8	10.5	8.8	8.7	14.1	17.8	25.9	27.4	30	18.2	
Min max dif	9.1	6.2	5.5	6.6	3.2	4.3	3.5	7.1	5.7	7.6	7.9	7.9	2.7	6.2
Southeast Victoria, Mount Burnett, 1990 - 2020 (3 km to Chromosol paddocks)														
Mean	23.6	20.5	15.8	10.7	7.3	5.9	6.6	9.3	12.6	16.9	20.5	22.8	14.4	
Lowest	20.3	17.2	11.8	8.8	6.2	4.7	5.2	7.8	9.8	14.3	17.6	19.6	13.3	
Highest	28.7	24	18.9	13.1	8.5	7	7.7	13.1	14.7	21.8	24.3	26.4	15.7	
Min max dif	8.4	6.8	7.1	4.3	2.3	2.3	2.5	5.3	4.9	7.5	6.7	6.8	2.4	5.4

Table S2. Raw sample data of dieldrin loss (%) and concentration (µg g^{-1}), resistant organic carbon (ROC), humus (HUM), particulate organic carbon (POC), carbon-to-nitrogen ratio (C:N), hydrogen-to-carbon ratio (H:C) and amplicon sequence variants (ASV). Units for carbon fractions are mg g^{-1} soil.

											Bacteria		Fungi	
ID	**Soil**	**Paddock**	**Farm**	**Dloss**	**Dieldrin**	**ROC**	**HUM**	**POC**	**C:N**	**H:C**	**Reads**	**ASVs**	**Reads**	**ASVs**
1	Kurosol	1	A	81	0.10	10.0	24.5	2.7	10.9	0.33	50,248	1,669	9,621	369
2	Kurosol	1	A	81	0.22	9.9	22.7	3.9	10.5	0.44	40,833	1,373	7,188	322
3	Kurosol	1	A	81	0.18	8.7	22.2	4.5	10.7	0.34	69,360	1,990	12,496	408
4	Kurosol	2	A	72	0.24	9.9	24.4	4.2	10.6	0.34	57,598	1,457	11,028	392
5	Kurosol	2	A	72	0.26	10.2	25.1	7.1	10.5	0.34	62,574	1,631	11,100	383
6	Kurosol	2	A	72	0.24	9.9	24.9	3.7	10.5	0.34	59,044	1,453	15,536	444
7	Kurosol	3	A	74	0.12	9.3	23.8	3.6	11.3	0.31	80,603	1,775	17,174	386
8	Kurosol	3	A	74	0.13	10.7	25.2	4.9	11.1	0.36	97,800	2,107	17,127	423
9	Kurosol	3	A	74	0.17	11.1	26.1	4.5	11.1	0.32	123,304	2,373	19,237	495
10	Kurosol	4	A	67	0.16	7.6	19.4	3.7	11.4	0.29	58,555	1,732	8,922	309
11	Kurosol	4	A	67	0.18	8.0	18.8	3.1	12.1	0.29	53,432	1,558	12,912	314
12	Kurosol	4	A	67	0.18	8.3	20.5	3.6	12.3	0.27	111,989	2,296	12,134	390
13	Kurosol	5	B	66	0.22	10.6	18.1	2.8	11.8	0.30	32,146	1,289	16,639	398
14	Kurosol	5	B	66	0.26	11.4	19.3	1.8	11.7	0.32	33,654	1,214	16,468	340
15	Kurosol	5	B	66	0.17	11.5	17.3	3.1	11.3	0.32	35,760	1,306	13,905	302
16	Kurosol	6	B	67	0.12	12.2	20.7	3.3	11.9	0.29	31,428	1,239	11,354	362
17	Kurosol	6	B	67	0.14	10.0	16.3	3.2	12.2	0.28	29,974	1,119	13,597	345
18	Kurosol	6	B	67	0.12	11.7	17.8	4.4	11.0	0.28	42,253	1,366	15,512	381
19	Kurosol	7	C	85	0.04	6.2	12.3	4.0	9.9	0.37	38,564	1,651	10,392	340
20	Kurosol	7	C	85	0.04	8.9	16.7	3.3	10.5	0.30	NA	NA	10,916	371
21	Kurosol	7	C	85	0.03	7.5	13.9	3.1	10.3	0.30	37,725	1,714	14,854	397
22	Chromosol	8	D	28	0.65	22.4	33.4	3.1	15.1	0.29	39,619	1,273	13,920	258
23	Chromosol	8	D	28	0.66	25.2	36.4	4.2	14.6	0.29	43,285	1,237	13,768	333
24	Chromosol	8	D	28	0.72	23.5	35.9	3.4	14.1	0.26	72,192	1,645	11,411	318
25	Chromosol	9	D	61	0.87	23.6	43.1	6.5	12.5	0.31	52,669	1,427	15,508	395
26	Chromosol	9	D	61	0.76	21.8	33.7	4.8	14.6	0.30	34,178	1,247	11,031	340
27	Chromosol	9	D	61	0.88	26.8	39.8	7.2	13.7	0.30	47,347	1,421	12,505	330
28	Chromosol	10	D	28	0.67	22.0	35.8	3.1	15.0	0.29	38,451	1,314	10,984	326
29	Chromosol	10	D	28	0.64	20.2	34.2	4.4	14.4	0.30	33,370	1,123	11,171	276
30	Chromosol	10	D	28	0.63	20.6	33.2	2.9	16.0	0.30	42,503	1,285	18,016	343
31	Chromosol	11	E	50	1.30	19.2	31.6	3.9	13.2	0.29	49,227	1,437	16,062	435
32	Chromosol	11	E	50	1.07	19.3	31.4	2.8	14.3	0.29	45,076	1,332	12,728	373
33	Chromosol	11	E	50	1.10	18.2	27.1	1.7	14.2	0.32	37,828	1,225	14,228	405
34	Chromosol	12	E	43	1.90	18.1	30.6	2.2	14.7	0.30	39,199	1,290	13,409	352
35	Chromosol	12	E	43	1.85	17.6	31.7	3.3	14.4	0.28	49,475	1,390	14,090	338
36	Chromosol	12	E	43	1.85	20.9	33.6	2.7	14.4	0.27	47,692	1,402	13,752	406

Table S3. Comparison of relative abundances and relative frequencies of bacteria and fungi in module zero and four of the network analysis.

	Abundances (%)			ASV frequencies (%)		
Samples	**Bacteria**	**Fungi**	**Archaea**	**Bacteria**	**Fungi**	**Archaea**
All samples	79.5	19.8	0.7	82.2	17.4	0.4
Kurosol	81.6	17.7	0.7	83.0	16.6	0.4
Kurosol, Module 0	77.7	18.9	3.4	82.8	15.7	1.5
Kurosol, Module 4	69.5	30.5	0.0	78.6	21.4	0.0
Chromosol	76.5	22.9	0.6	81.3	18.5	0.3

Table S4. Phylofactor model coefficient and F statistic with dieldrin loss as numeric predictor for the aggregated presence of taxonomic groups. The resulting clades had a higher probability to be present in high dieldrin-loss environments (phylofactor mixed algorithm)

	Phylum	n	Coefficient	df	F value	*p*	Phylofactor	Group
Chromosol & Kurosol								
	Chloroflexi	33	0.34	1	394.62	< 0.001	1	6-member Monophyletic clade
	Planctomycetes	33	0.1	1	386.81	< 0.001	2	17-member Monophyletic clade
	Actinobacteria	33	0.07	1	371.41	< 0.001	3	18-member Monophyletic clade
	Acidobacteria	33	0.05	1	353.25	< 0.001	4	29-member Monophyletic clade
	Bacteroidetes	33	0.13	1	329.44	< 0.001	5	17-member Monophyletic clade
Kurosol								
	Bacteroidetes	18	0.33	1	186.88	< 0.001	1	55-member Monophyletic clade
	Firmicutes	18	0.19	1	142.1	< 0.001	2	44-member Monophyletic clade
	Actinobacteria	18	0.05	1	116.13	< 0.001	3	589-member Monophyletic clade
	Proteobacteria	18	0.16	1	40.73	< 0.001	4	24-member Monophyletic clade
	Chloroflexi	18	0.14	1	32.66	< 0.001	5	27-member Monophyletic clade
Chromosol								
	Acidobacteria	15	-0.21	1	0.01	0.93	1	2-member Monophyletic clade
	Acidobacteria	15	0.04	1	0.00	0.97	2	19-member Monophyletic clade
	Actinobacteria	15	0.06	1	0.11	0.74	3	8-member Monophyletic clade
	Acidobacteria	15	0.05	1	0.31	0.58	4	15-member Monophyletic clade
	Actinobacteria	15	0.18	1	0.70	0.4	5	2-member Monophyletic clade